Contribution from the Department of Chemistry and Laboratory for Molecular Structure and Bonding, Texas A&M University, College Station, Texas 77843

New Di- and Trinuclear Complexes of Ruthenium with Octahedra Joined on Faces or Edges. 2.[1] New Compounds with $Ru^{II}Ru^{II}$, $Ru^{II}Ru^{III}$, and $Ru^{III}Ru^{III}$ in Face-Sharing Bioctahedra: Structures, Magnetism, and Electrochemistry

F. Albert Cotton* and Raymund C. Torralba

Received September 25, 1990

Five new compounds containing face-sharing bioctahedral diruthenium molecules have been prepared and studied by X-ray crystallography, EPR spectroscopy, cyclic voltammetry, and magnetic susceptibility measurements. These compounds and the principal data concerning them are as follows: $[Ru_2Cl_3(PBu_3)_6][RuCl_4(PBu_3)_2]$ (**1a**), monoclinic, space group $I2/a$, a = 31.971 (6) Å, b = 14.247 (3) Å, c = 26.624 (7) Å, β = 107.1467 (4)°, V = 11,588 (9) Å^3, Z = 4, Ru-Ru distance = 3.395 (1) Å, μ_{eff} = 2.05 μ_B, $g_\perp$ = 2.42, $g_\parallel$ = 1.58, undergoes oxidation at +1.39 and +0.90 V; $[Ru_2Cl_3(PBu_3)_6][BPh_4]$ (**1b**), monoclinic, space group $P2/a$, a = 27.87 (1) Å, b = 13.444 (9) Å, c = 28.011 (5) Å, β = 98.50 (3)°, V = 10,382 (14) Å^3, Z = 4, Ru-Ru distance = 3.412 (1) Å, μ_{eff} = 1.1 μ_B; $Ru_2Cl_5(PBu_3)_4$ (**2**), monoclinic, space group $P2_1/a$, a = 19.034 (9) Å, b = 13.407 (5) Å, c = 25.51 (1) Å, β = 100.74 (5)°, V = 6395 (10) Å^3, Z = 4, Ru-Ru distance = 3.279 (2) Å, μ_{eff} = 1.95 μ_B/molecule, $g_\perp$ = 2.44, $g_\parallel$ = 1.59, undergoes oxidation at +0.95 V and reduction at -0.73 V; $Ru_2Cl_5(PMe_2Ph)_4$ (**3**), monoclinic, space group $C2/c$, a = 15.873 (4) Å, b = 11.216 (2) Å, c = 21.312 (5) Å, β = 101.65 (3)°, V = 3716 (3) Å^3, Z = 4, Ru-Ru distance = 2.9941 (4) Å, μ_{eff} = 1.94 μ_B/molecule, g_1 = 2.33, g_2 = 2.06, g_3 = 1.87, undergoes oxidation at +0.55 V and reduction at -0.09 V; $Ru_2Cl_5(PMe_3)_4$ (**4**), monoclinic, space group $P2_1$, a = 9.232 (4) Å, b = 12.790 (9) Å, c = 10.967 (5) Å, β = 95.4491 (7)°, V = 1289 (2) Å^3, Z = 2, Ru-Ru distance = 2.992 (1) Å, g_1 = 2.29, g_2 = 2.07, g_3 = 1.90, undergoes oxidation at +0.58 V and reduction at -0.18 V; $Ru_2Cl_6(PEt_3)_3$ (**5**), triclinic, space group $P\bar{1}$, a = 11.211 (4) Å, b = 17.387 (5) Å, c = 7.993 (3) Å, α = 93.53 (3)°, β = 91.93 (3)°, γ = 95.91 (3)°, V = 1533.9 (2) Å^3, Z = 2, Ru-Ru distance = 3.201 (1) Å, μ_{eff} = 1.91 μ_B/Ru. It is shown that on the basis of all the data for these and seven previously reported chlorophosphine compounds the following conclusions can be drawn. In compounds **1a** and **1b**, as well as in three others of the same type with different PR_3 ligands, there is no Ru-Ru bonding. In compound **2** and its PEt_2Ph analogue, where the phosphine ligands are unsymmetrically distributed, there is valence trapping and no Ru-Ru bonding. In the compounds with symmetrically distributed phosphines, such as **3** and **4**, the odd electron is delocalized and there is a weak Ru-Ru bond (formal bond order $^1/_2$). Finally, in the Ru^{III},Ru^{III} type compounds such as **5**, there is essentially no Ru-Ru bond.

Introduction

The study of di- and trinuclear complexes of ruthenium with average formal oxidation states in the range +2 to +3 has a substantial previous history, references to which may be found in our previous paper[1] and in standard compendia.[2,3] In this paper, we present the results of an extensive study of dinuclear face-sharing bioctahedral (FSBO) type compounds in which the formal oxidation numbers run from II,II through II,III to III,III. One of the main contributions of this paper is to supply needed structural data on such compounds, such data having been notably exiguous in the past compared to the relative abundance of magnetic (including EPR) and electrochemical data. We now add six new structures to the seven[1,4-9] previously available for compounds containing Cl and phosphines as ligands as well as much new magnetic and electrochemical data. On the basis of all the available data, we shall discuss the electronic structures of these compounds. The principal questions concern whether Ru-Ru bonding occurs or whether there is valence-state localization in the II,III type compounds.

Experimental Section

All chemical reactions, unless otherwise stated, were done under an argon atmosphere employing standard vacuum-line techniques.[10] All solvents were predried over molecular sieves and freshly distilled under nitrogen prior to use. CH_2Cl_2 was distilled over P_2O_5; benzene, *n*-hexane, and diethyl ether were distilled from Na-K/benzophenone; ethanol and methanol were distilled from Mg. $RuCl_3 \cdot 3H_2O$ was purchased from Aldrich Chemical Co. and was either used as received or heated under vacuum for 1 h before mixing it with other chemicals. PBu_3, PEt_3, PMe_3, and PMe_2Ph (Strem Chemicals) were transferred into Schlenk tubes and kept under argon. These were stored in the refrigerator when not in use. $(C_4H_9N)_4PF_6$ (Aldrich) was recrystallized before use. $NaBPh_4$, purchased from Sigma Chemical Co., was used as received.

The electronic absorption spectra in CH_2Cl_2 were recorded on a Cary 17D spectrophotometer. Cyclic voltammetric studies were carried out by using a BAS 100 electrochemical analyzer. All CV studies were done in CH_2Cl_2 solutions with $(C_4H_9)_4NPF_6$ as supporting electrolyte and Ag/AgCl as reference electrode. The scan rate used for all reported results was 100 mV/s. Under these conditions, Cp_2Fe had $E_{1/2}$ at 0.42-0.47 V.

Magnetic susceptibilities of the solid bulk samples for compounds **1a**, **1b**, **2**, **3**, and **4** were obtained by the Guoy method using a Johnson Matthey magnetic balance. For a CH_2Cl_2 solution of compound **5**, the Evans method[11] was used employing a EM390 NMR spectrometer at 90 MHz. ESR spectra of frozen CH_2Cl_2-toluene solutions were recorded at 77 K by an IBM Instruments, Inc., ER200D-SRC spectrometer equipped with a Bruker ER082(155/45) magnet.

Preparation of $[Ru_2Cl_3(PBu_3)_6][Y]$. (a) Y = $RuCl_4(PBu_3)_2$ (1a). A 0.305-g (1.16-mmol) sample of $RuCl_3 \cdot 3H_2O$ was dissolved in 1.5 mL of ethanol and 0.73 g (3.61 mmol) of PBu_3 was added dropwise. The mixture was stirred for 2 h, left undisturbed, and then exposed to air after 3 days. Large red crystals of **1a** were deposited at the bottom of the reaction flask within 5 days of exposure to air. These were washed with small amounts (2 × 2 mL) of ethanol followed by diethyl ether and dried in air. The yield was 75%. The electronic absorption spectrum had maxima at 330 nm ($\epsilon = 0.56 \times 10^3$ cm^{-1} M^{-1}), 370 nm ($\epsilon = 1.05 \times 10^3$ cm^{-1} M^{-1}), 380 nm ($\epsilon = 1.02 \times 10^3$ cm^{-1} M^{-1}), and 500 nm ($\epsilon = 0.12 \times 10^3$ cm^{-1} M^{-1}).

(b) Y = BPh_4^- (1b). $[Ru_2Cl_3(PBu_3)_6][BPh_4]$ was prepared quantitatively from **1a** by ion exchange using an excess of $NaBPh_4$. A 0.1-g sample of **1a** was dissolved in methanol. A yellow precipitate immediately formed upon the addition of $NaBPh_4$. This was filtered, washed with methanol (2 × 3 mL), and dried in air. The yield was 0.078 g (92.1%). Recrystallization was carried out by layering a benzene solution of this dinuclear compound with twice its volume of *n*-hexane. The electronic absorption spectrum had maxima at 335 nm ($\epsilon = 2.19 \times 10^3$ cm^{-1} M^{-1}) and 375 nm ($\epsilon = 1.59 \times 10^3$ cm^{-1} M^{-1}).

(1) Part 1: Cotton, F. A.; Torralba, R. C.; Matusz, M. *Inorg. Chem.* **1989**, *28*, 1516.
(2) Wilkinson, G., Ed. *Comprehensive Coordination Chemistry*; Pergamon Press: New York, 1987; Vol. 4, p 572.
(3) Seddon, E. A.; Seddon, K. R. *The Chemistry of Ruthenium*; Elsevier: New York, 1984; pp 310, 487-515.
(4) Statler, J. A.; Wilkinson, G.; Thornton-Pett, M.; Hursthouse, M. B. *J. Chem. Soc., Dalton Trans.* **1984**, 1731.
(5) Laing, M.; Pope, L. *Acta Crystallogr.* **1976**, *B32*, 1547.
(6) Raspin, K. A. *J. Chem. Soc. A* **1969**, 461.
(7) Alcock, N. W.; Raspin, K. A. *J. Chem. Soc. A* **1968**, 2108.
(8) Contreras, R.; Elliot, G. G.; Gould, R. O.; Heath, G. A.; Lindsay, A. J.; Stephenson, T. A. *J. Organomet. Chem.* **1981**, *215*, C6-C10.
(9) Chioccola, G.; Daly, J. J. *J. Chem. Soc. A* **1968**, 1981.
(10) Shriver, D. F.; Drezden, M. A. *The Manipulation of Air-Sensitive Compounds*, 2nd ed.; Wiley: New York, 1986.
(11) Evans, D. F. *J. Chem. Soc.* **1959**, 2003.

0020-1669/91/1330-2196$02.50/0

Table I. Crystal Data for Compounds **1a** and **1b**

	1a	**1b**
formula	$Ru_3Cl_7P_8C_{96}H_{216}$	$Ru_2Cl_3P_6C_{96}BH_{182}$
fw	2169.96	1841.68
space group	$I2/a$	$P2/a$
syst abs	hkl, $h + k + l = 2n + 1$	$h0l$, $h = 2n + 1$
a, Å	31.971 (6)	27.87 (1)
b, Å	14.247 (3)	13.444 (9)
c, Å	26.624 (7)	28.011 (5)
α, deg	90	90
β, deg	107.1467 (4)	98.50 (3)
γ, deg	90	90
V, Å	11,588 (9)	10,382 (14)
Z	4	4
d_{calc}, g/cm	1.244	1.178
cryst size, mm	0.35 × 0.15 × 0.20	0.30 × 0.20 × 0.40
μ(Mo Kα), cm^{-1}	6.882	4.928
data collcn instrum	Enraf-Nonius CAD4S	Enraf-Nonius CAD4S
radiation (monochromated in incident beam)	Mo Kα (λ_α = 0.71073 Å)	Mo Kα (λ_α = 0.71073 Å)
orientation reflcns: no.; range (2θ), deg	22; $21 < 2\theta < 29$	24; $20 < 2\theta < 28$
temp, °C	−80 ± 1	−80 ± 1
scan method	2θ–ω	ω
data collcn range (2θ), deg	$4 < 2\theta < 45$	$4 < 2\theta < 50$
no. of unique data, tot. no. with $F_0 > 3\sigma(F_0)$	7556, 4649	18246, 9440
no. of params refined	516	929
transm factors, %: max, min	1.00, 0.91	1.00, 0.966
R^a	0.0548	0.0670
R_w^b	0.0688	0.0886
quality-of-fit indicator^c	1.698	1.824
largest shift/esd, final cycle	0.20	0.379
largest peak, e/Å^3	0.47	1.371

$^a R = \sum||F_o| - |F_c||/\sum|F_o|$. $^b R_W = [\sum w(|F_o| - |F_c|)/\sum w|F_o|]^{1/2}$; $w = 1/\sigma(|F_o|)$. ^{c}Quality-of-fit = $[\sum w(|F_o| - |F_c|)/(N_{observns} - N_{params})]^{1/2}$.

Preparation of $Ru_2Cl_5(PBu_3)_4$ (2). The process described by Nicholson[12] was repeated and confirmed to proceed substantially as he reported it. We have previously described a modified procedure for obtaining pure $Ru_2Cl_6(PBu_3)_4$,[1] one of his products. Prolonged exposure of the reaction mixture to air, however, produced green, red, and brown crystals later identified by X-ray crystallography as $[Ru_3Cl_6(PBu_3)_6]$-$[RuCl_4(PBu_3)_2]$[13] (yield = 14%), **1a** (yield = 7%), and $Ru_2Cl_6(PBu_3)_4$ (yield = 20%), respectively. The mother liquor left after isolating the initial solid products deposited green crystals of **2** within 2 days (yield = 13%). These crystals were the structural isomer of the previously reported dark red $Ru_2Cl_5(PBu_3)_4$.[9] The electronic absorption spectrum had maxima at 360 nm ($\epsilon = 4.35 \times 10^3$ cm^{-1} M^{-1}; shoulder at 340 nm), 410 nm ($\epsilon = 2.66 \times 10^3$ cm^{-1} M^{-1}), and 700 nm ($\epsilon = 1 \times 10^3$ cm^{-1} M^{-1}; broad).

Preparation of $Ru_2Cl_5(PMe_2Ph)_4$ (3). A 0.30-g (1.16-mmol) sample of $RuCl_3 \cdot 3H_2O$ was dissolved in 2 mL of methanol, and 0.34 g (2.46 mmol) of PMe_2Ph was added. A dark-precipitate immediately formed. The solid material, 0.41 g (yield = 75.8%), was isolated by filtration after 2 h more of stirring. A 0.1-g sample of the crude product was recrystallized by layering its CH_2Cl_2 solution with 2–3 times its volume of methanol or diethyl ether. Large, dark red crystals of **3** formed within 2–3 days.

Preparation of $Ru_2Cl_5(PMe_3)_4$ (4). Compound **4** formed as a side product in the synthesis of $Ru_3Cl_8(PMe_3)_4$.[14] A 0.61-g (2.33-mmol) sample of $RuCl_3 \cdot 3H_2O$ was dissolved in 2.5 mL of methanol, and 0.24 g of (3.11 mmol) PMe_3 was added dropwise. The reaction mixture was stirred for 2 h and left undisturbed. After 8 days, dark green crystals had deposited. These were recovered by filtration in air, washed with methanol (2 × 5 mL), and dried either in air or under vacuum. Yields ranged from 38% to 56%. The crude product, after recrystallization, was found to have no more than 4% of $Ru_2Cl_5(PMe_3)_4$ (**4**) in most of the trials that were carried out. Recrystallization was done by layering a CH_2Cl_2 solution of the crude product with 2–3 times its volume of benzene. The crystals of $Ru_2Cl_5(PMe_3)_4$ were readily discernible under the microscope as dark brown-red prisms and this allowed their separation from the triruthenium complex to be done manually in most trials.

Preparation of $Ru_2Cl_6(PEt_3)_3$ (5). A 0.6-g (2.33-mmol) sample of $RuCl_3 \cdot 3H_2O$ was dissolved in 3 mL of ethanol and 0.67 g (5.65 mmol) of PEt_3 was added. The mixture was stirred for 2 h and then left undisturbed. After 3 days, a large amount of dark brown solid formed. This was filtered in air, washed with ethanol (2 × 2 mL), and either vacuum- or air-dried. The yield was 0.44 g. $Ru_3Cl_8(PEt_3)_4$ was determined to be present as an impurity on the basis of the electronic absorption spectrum (maxima at 335, 410, 495, and 830–840 nm). In all the trials when the crude product was recrystallized, $Ru_2Cl_6(PEt_3)_3$ was obtained in reasonable yields (at least 40%). The electronic absorption spectrum of this diruthenium complex had maxima at 360, 420, and 500 nm. In a few instances, $Ru_3Cl_8(PEt_3)_4$ was also recrystallized since the crude product contained a small amount of it. Recrystallization was carried out in a couple of ways for this case: (a) slow diffusion of ether vapor into a CH_2Cl_2 solution of the crude product; (b) layering the CH_2Cl_2 solution with ether or *n*-hexane.

X-ray Crystallography. For each of the compounds, the structure determination was carried out by employing procedures routine in this laboratory.[15] Relevant crystallographic data and results of the refinement are summarized in Tables I–III. The final thermal parameters and bond distances and angles for each structure are available in the Supplementary Material.

For **1a**, the crystal system was found to be monoclinic, and oscillation photographs confirmed the body centering and the Laue group ($2/m$). Systematic conditions observed in the data set indicated either $I2/a$ or Ia as the space group. Heavy atoms were located by direct methods and were consistent with $I2/a$. This was assumed in preference to Ia and allowed for satisfactory refinement. The other non-hydrogen atoms were located by an alternating series of Fourier maps and least-squares refinement cycles. The δ-carbon atoms in the *n*-butyl groups had generally high thermal displacement parameters, but no disorder was directly observed. Hydrogen atoms were not included in the model. Table IV lists the final positional parameters and isotropic-equivalent thermal displacement parameters.

For **1b**, preliminary examination of the crystal revealed that the crystal system was monoclinic with a primitive lattice. Oscillation photographs confirmed these and the Laue group ($2/m$). Systematic conditions in the data set indicated either $P2/a$ or Pa as the space group. The structure was partially solved when the heavy atoms were found by direct methods.

(12) Nicholson, J. K. *Angew. Chem., Int. Ed. Engl.* **1967**, *6*, 264.
(13) This triruthenium compound will be discussed in a separate paper (Part 4 of this series).
(14) The triruthenium compounds will be discussed in a separate paper (Part 3 of this series).
(15) The calculations were done on a MicroVax II computer with an SDP package software. ψ-Scan absorption corrections were made: North, A. C. T.; Phillips, D. C.; Matthews, F. S. *Acta Crystallogr.* **1968**, *A24*, 351. Structure solutions employed SHELXS-86 and SHELX-76; Sheldrick, G. M. SHELXS-86, Institut fur Anorganische Chemie der Universitat, Göttingen, FRG, 1986. Sheldrick, G. M. SHELX-76. Program for Crystal Structure Determination. University of Cambridge, Cambridge, England, 1976.

Table II. Crystal Data for Compounds **2–4**

	2	**3**	**4**
formula	$Ru_2Cl_5P_4C_{48}H_{108}$	$Ru_2Cl_5P_4C_{32}H_{44}$	$Ru_2Cl_5P_4C_{12}H_{36}$
fw	1188.7	932.01	683.72
space group	$P2_1/a$	$C2/c$	$P2_1$
syst abs	$h0l$, $h = 2n + 1$ $0k0$, $k = 2n + 1$	hkl, $h + k = l = 2n + 1$ $h0l$, $h, l = 2n + l$	$0k0$, $k = 2n + 1$
a, Å	19.034 (9)	15.873 (4)	9.232 (4)
b, Å	13.407 (5)	11.216 (2)	12.790 (9)
c, Å	25.51 (1)	21.312 (5)	10.967 (5)
α, deg	90	90	90
β, deg	100.74 (5)	101.65 (3)	95.4491 (7)
γ, deg	90	90	90
V, Å^3	6395 (10)	3716 (3)	1289 (2)
Z	4	4	2
d_{calc}, g/cm^3	1.235	1.679	1.762
cryst size, mm	0.35 × 0.25 × 0.40	0.30 × 0.08 × 0.18	0.28 × 0.08 × 0.20
μ(Mo Kα), cm^{-1}	7.998	13.642	18.991
data collcn instrum	Enraf-Nonius CAD4S	Enraf-Nonius CAD4S	Enraf-Nonius CAD4S
radiation (monochromated in incident beam)	Mo Kα (λ_α = 0.710 73 Å)	Mo Kα	Mo Kα
orientation reflcns: no.; range (2θ), deg	25; $5 < 2\theta < 26$	25; $14 < 2\theta < 35$	25; $14 < 2\theta < 28$
temp, °C	21 ± 1	−40 ± 1	−80 ± 1
scan method	ω	ω	ω
data collcn range (2θ), deg	$4 < 2\theta < 50$	$4 < 2\theta < 50$	$4 < 2\theta < 55$
no. of unique data, tot. no. with $F_o^2 > 3\sigma(F_o^2)$	8021, 2474	3253, 2449	3081, 2757
no. of params refined	533	263	208
transm factors, %: max, min	0.999, 0.972	0.998, 0.902	0.997, 0.908
R^a	0.0663	0.0278	0.0308
$R_w{}^b$	0.0797	0.0412	0.0409
quality-of-fit indicator^c	1.572	1.181	1.11
largest shift/esd, final cycle	0.22	0.88	0.46
largest peak, e/Å^3	0.404	0.510	0.871

$^a R = \sum||F_o| - |F_c||/\sum|F_o|$. $^b R_w = [\sum w(|F_o| - |F_c|)/\sum w|F_o|]^{1/2}$; $w = 1/\sigma(|F_o|)$. ^{c}Quality-of-fit = $[\sum w(|F_o| - |F_c|)/(N_{observns} - N_{params})]^{1/2}$.

Table III. Crystal Data for Compound **6**

formula	$Ru_2Cl_6P_3C_{18}H_{45}$
fw	769.34
space group	$P\bar{1}$
syst abs	none
a, Å	11.211 (4)
b, Å	17.387 (5)
c, Å	7.933 (3)
α, deg	93.53 (3)
β, deg	91.93 (3)
γ, deg	95.91 (3)
V, Å	1533.9 (2)
Z	2
d_{calc}, g/cm	1.666
cryst size, mm	0.27 × 0.04 × 0.12
μ(Mo Kα), cm^{-1}	16.569
data collcn instrum	Rigaku AFC5R
radiation (monochromated in incident beam)	Mo Kα (λ_α = 0.710 73 Å)
orientation reflcns: no.; range (2θ), deg	25; $18 < 2\theta < 29$
temp, °C	21 ± 1
scan method	2θ–ω
data collcn range (2θ), deg	$4 < 2\theta < 55$
no. of unique data, tot. no. with $F_o > 3\sigma(F_o)$	5403, 3442
no. of params refined	262
transm factors, %: max, min	1.00, 0.884
R^a	0.0425
$R_w{}^b$	0.0596
quality-of-fit indicator^c	1.306
largest shift/esd, final cycle	0.0
largest peak, e/Å^3	0.714

$^a R = \sum||F_o| - |F_c||/\sum|F_o|$. $^b R_w = [\sum w(|F_o| - |F_c|)/\sum w|F_o|]^{1/2}$; $w = 1/\sigma(|F_o|)$. ^{c}Quality-of-fit = $[\sum w(|F_o| - |F_c|)/(N_{observns} - N_{params})]^{1/2}$.

They were consistent with $P2/a$, which was assumed (in preference over Pa) and allowed for satisfactory refinement. The rest of the non-hydrogen atoms were located by an alternating series of Fourier maps and least-squares refinement cycles. The γ- and δ-carbon atoms in the n-butyl groups of the phosphine ligands had generally high thermal displacement parameters and tended to give unacceptable C–C distances. This problem is typical of structures containing relatively long alkyl chains. The C–C distances were constrained to correspond to 1.5 Å while all the phenyl carbons were constrained to form a regular hexagon. The model was refined without the hydrogen atoms. Table V lists the final positional and isotropic-equivalent thermal displacement parameters.

For **2**, preliminary examination of the crystal revealed that the crystal system was monoclinic, the lattice was primitive, and the Laue group was $2/m$. Data collection results had systematic absences indicating that the space group was $P2_1/a$. The structure was partially solved when the Ru, Cl, and P atoms were found by using the Patterson heavy-atom method (SHELXS86). The rest of the non-hydrogen atoms were located by an alternating series of Fourier maps and least-squares refinement cycles. The model was refined to convergence with all the atoms having anisotropic thermal parameters. However, some of the carbon atoms in the n-butyl groups of the phosphine ligand had high thermal displacement parameters, and several of the C–C distances were unacceptably long. The R value at that point was 0.062 (R_w = 0.070) and the quality of fit for the model was 1.811. The C–C distances were constrained to correspond to 1.5 Å, and the new model refined to convergence (SHELX76). The final residuals were R = 0.0663 (R_w = 0.0797); quality of fit = 1.572. Hydrogen atoms were not included in the refined model. Table VI lists the final positional and isotropic-equivalent thermal displacement parameters.

For **3**, preliminary examination revealed that the crystal system was monoclinic with a c-centered lattice. Oscillation photographs confirmed that the crystal was indeed c-centered and the Laue group was $2/m$. The systematic conditions observed indicated either $C2/c$ or Cc as the space group. The former was assumed, and the heavy atoms found by direct methods were consistent with it. Several phenyl carbon atoms were also found together with the heavier atoms. These were allowed to refine satisfactorily. The remaining carbon atoms were located by an alternating series of Fourier maps and least-squares refinement cycles. After all the non-hydrogen atoms were refined with anisotropic thermal displacement parameters, hydrogen atoms were added in calculated positions. The model was refined with the phenyl hydrogens constrained to have the same isotropic thermal displacement parameter and the methyl hydrogens also constrained to have the same isotropic thermal displacement parameter. Table VII lists the final positional and isotropic-equivalent thermal displacement parameters.

For **4**, preliminary examination revealed that the crystal system was monoclinic with a primitive lattice. Oscillation photographs confirmed this and showed that the Laue group was $2/m$. The systematic absences indicated as possible space groups: $P2_1/m$ or $P2_1$. First, $P2_1/m$ was assumed, and direct methods were used to find the heavy atoms. How-

Table IV. Positional and Isotropic-Equivalent Thermal Displacement Parameters (B_{iso} in Å^2) for $[Ru_2Cl_3(PBu_3)_6][RuCl_4(PBu_3)_2]$[a]

atom	x	y	z	B_{iso}
Ru(1)	0.30405 (2)	0.48015 (5)	0.03390 (3)	1.76 (1)
Ru(2)	0.500	0.000	0.000	2.47 (2)
Cl(1)	0.250	0.3518 (2)	0.000	2.19 (7)
Cl(2)	0.23766 (7)	0.5408 (2)	0.05358 (8)	2.20 (5)
Cl(3)	0.45877 (9)	0.1389 (2)	−0.0048 (1)	3.73 (6)
Cl(4)	0.43926 (8)	−0.0907 (2)	0.0051 (1)	3.62 (6)
P(1)	0.34290 (8)	0.6190 (2)	0.05044 (9)	2.19 (5)
P(2)	0.35547 (7)	0.3978 (2)	0.00754 (9)	2.10 (5)
P(3)	0.32532 (8)	0.4294 (2)	0.11927 (9)	2.28 (5)
P(4)	0.47557 (8)	−0.0161 (2)	−0.0929 (1)	2.99 (6)
C(1)	0.3935 (3)	0.6226 (8)	0.1075 (4)	3.3 (2)
C(2)	0.4340 (4)	0.677 (1)	0.1035 (5)	6.1 (4)
C(3)	0.4744 (4)	0.652 (2)	0.1524 (6)	10.8 (5)
C(4)	0.5151 (6)	0.681 (2)	0.1398 (8)	11.2 (7)
C(5)	0.3627 (3)	0.6696 (7)	−0.0025 (4)	2.8 (2)
C(6)	0.3294 (4)	0.7230 (8)	−0.0470 (4)	4.4 (3)
C(7)	0.3519 (4)	0.7555 (8)	−0.0877 (4)	4.4 (3)
C(8)	0.3208 (4)	0.805 (1)	−0.1352 (5)	6.1 (4)
C(9)	0.3098 (3)	0.7157 (7)	0.0651 (4)	3.7 (3)
C(10)	0.3342 (4)	0.8098 (8)	0.0779 (5)	5.0 (3)
C(11)	0.3023 (5)	0.8867 (9)	0.0858 (5)	5.9 (4)
C(12)	0.2937 (5)	0.874 (1)	0.1364 (5)	7.4 (4)
C(13)	0.4128 (3)	0.4342 (7)	0.0346 (4)	2.5 (2)
C(14)	0.4467 (3)	0.3864 (7)	0.0110 (4)	3.2 (2)
C(15)	0.4940 (3)	0.3952 (8)	0.0520 (4)	3.3 (2)
C(16)	0.5294 (3)	0.3568 (8)	0.0293 (4)	3.8 (3)
C(17)	0.3481 (3)	0.3889 (7)	−0.0634 (4)	2.9 (2)
C(18)	0.3585 (3)	0.4758 (7)	−0.0916 (4)	3.3 (2)
C(19)	0.3581 (4)	0.4461 (9)	−0.1483 (4)	5.6 (3)
C(20)	0.3744 (6)	0.527 (1)	−0.1756 (5)	9.2 (5)
C(21)	0.3598 (3)	0.2706 (6)	0.0257 (4)	2.7 (2)
C(22)	0.3313 (4)	0.2021 (7)	−0.0155 (4)	3.6 (3)
C(23)	0.3369 (4)	0.1017 (7)	0.0076 (4)	4.2 (3)
C(24)	0.3065 (4)	0.0305 (8)	−0.0306 (5)	5.3 (3)
C(25)	0.2899 (3)	0.3362 (7)	0.1328 (4)	3.2 (2)
C(26)	0.2996 (5)	0.2369 (9)	0.1195 (5)	6.1 (4)
C(27)	0.2716 (5)	0.1639 (9)	0.1424 (5)	6.7 (4)
C(28)	0.2879 (7)	0.153 (1)	0.2034 (6)	9.9 (6)
C(29)	0.3819 (3)	0.3863 (7)	0.1511 (4)	3.1 (2)
C(30)	0.3915 (4)	0.358 (1)	0.2108 (5)	6.6 (4)
C(31)	0.4369 (5)	0.323 (2)	0.2328 (6)	11.7 (6)
C(32)	0.4704 (6)	0.346 (2)	0.2174 (8)	18 (1)
C(33)	0.3209 (3)	0.5228 (7)	0.1667 (4)	3.1 (2)
C(34)	0.2829 (3)	0.5194 (8)	0.1899 (4)	4.0 (2)
C(35)	0.2807 (4)	0.6097 (8)	0.2202 (4)	4.7 (3)
C(36)	0.2433 (5)	0.609 (1)	0.2439 (5)	6.3 (3)
C(37)	0.5151 (4)	0.0161 (8)	−0.1284 (4)	4.4 (3)
C(38)	0.5522 (4)	−0.056 (1)	−0.1217 (5)	5.5 (3)
C(39)	0.5870 (4)	−0.020 (1)	−0.1473 (6)	10.8 (5)
C(40)	0.5796 (7)	−0.028 (2)	−0.1958 (7)	18.0 (7)
C(41)	0.4578 (3)	−0.1354 (7)	−0.1149 (4)	3.1 (2)
C(42)	0.4385 (4)	−0.1481 (8)	−0.1746 (4)	4.3 (3)
C(43)	0.4249 (4)	−0.2501 (8)	−0.1874 (4)	4.7 (3)
C(44)	0.4019 (5)	−0.2649 (9)	−0.2479 (4)	5.8 (4)
C(45)	0.4297 (3)	0.0587 (8)	−0.1286 (4)	3.7 (3)
C(46)	0.3864 (3)	0.0353 (9)	−0.1168 (5)	4.5 (3)
C(47)	0.3457 (4)	0.073 (1)	−0.1612 (5)	5.4 (3)
C(48)	0.3477 (5)	0.1787 (9)	−0.1687 (5)	6.7 (4)

[a] Values for anisotropically refined atoms are given in the form of the equivalent isotropic displacement parameter defined as $(4/3)[a^2B_{11} + b^2B_{22} + c^2B_{33} + ab(\cos\gamma)B_{12} + ac(\cos\beta)B_{13} + bc(\cos\alpha)B_{23}]$. The numbers in parentheses are the estimated standard deviations in the least significant digit.

ever, subsequent least-squares refinement and Fourier maps failed to show satisfactory behavior. The space group $P2_1$ was then used. The heavy atoms were found as before, and the remaining non-hydrogen atoms were located by an alternating series of Fourier maps and least-squares refinement cycles. Hydrogen atoms were excluded in the model. Table VIII lists the final positional and isotropic-equivalent thermal displacement parameters.

For **5**, preliminary examination revealed that the crystal system was triclinic and the Laue group was $\bar{1}$. The heavy atoms were found by direct methods and were consistent with space group $P\bar{1}$. This space group was assumed over $P1$ and allowed for satisfactory refinement. All

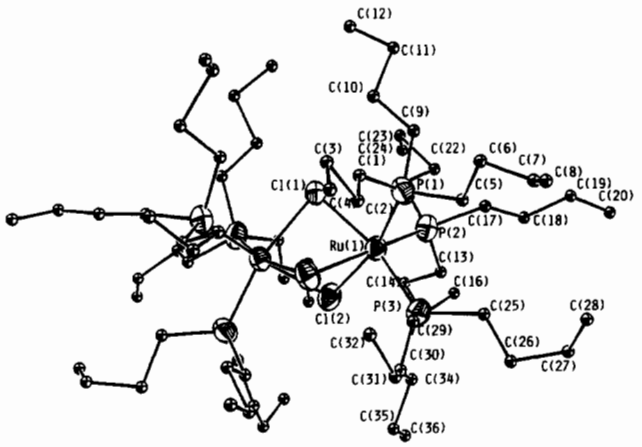

Figure 1. ORTEP drawing of the cation in compound **1a** and **1b**. A crystallographic 2-fold axis passing along Cl(1) perpendicular to the Ru–Ru vector relates each unlabeled atom to a labeled one. Carbon atoms were given arbitrary radii.

of the other non-hydrogen atoms were located by an alternating series of Fourier maps and least-squares refinement cycles. Hydrogen atoms were not included in the model. Table IX lists the final positional and isotropic-equivalent thermal displacement parameters.

Results

Preparative Chemistry. In the case of the Ru(II), Ru(II) face-sharing bioctahedral species, compounds **1a** and **1b**, the synthesis is similar to those for previously characterized complexes of the same $[Ru_2Cl_3L_6]^+$ type (L = tertiary monophosphine).[3,4,6] Whereas an excess of the phosphine and refluxing are employed in the latter, compounds **1a** and **1b** were prepared under milder conditions, that is, employing just the right stoichiometry and running the reaction at ambient temperatures over several days. As far as the Ru(II), Ru(III) type face-sharing bioctahedral complexes are concerned, the preparations were also done along traditional lines.[3,12] Compound **2** precipitated out as green crystals from the filtrate left from the isolation of $Ru_2Cl_6(PBu_3)_4$, $[Ru_3Cl_6(PBu_3)_6][RuCl_4(PBu_3)_2]$,[13] and **1a**. It was obviously different from its stereoisomer with C_2 symmetry[9] based on the color alone. Compound **3** was produced as insoluble brownish red crystals in methanol, together with the tiny green crystals of $Ru_3Cl_8(PMe_2Ph)_4$.[14] Compound **4** occurs as a side product in the synthesis of $Ru_3Cl_8(PMe_3)_4$.[14]

Structure and Bonding in the Ru(II), Ru(II) Compounds: $[Ru_2Cl_3(PBu_3)_6][Y]$, Y = $RuCl_4(PBu_3)_2^-$ (1a) or BPh_4^- (1b). The structures of the cations in these compounds are identical and this is shown in Figure 1. The important bond distances and angles for the central part of the cations are listed in Tables X and XI. In both cases, a crystallographically imposed 2-fold symmetry axis perpendicular to the metal–metal vector and containing Cl(1) relates each of the unlabeled atoms in the cation to an unlabeled one. The core has approximate D_{3h} symmetry with the principal axis passing along the metal–metal vector.

The structural features of compounds **1a** and **1b** are essentially the same as those for the previously characterized face-sharing bioctahedra of the $[L_3Ru^{II}Cl_3Ru^{II}L_3]^+$ type (L = PMe_3,[4] PMe_2Ph,[5] PEt_2Ph[6]). All of the Ru–Cl bonds trans to Ru–P bonds are relatively longer than the typical Ru–Cl bond lengths of 2.3–2.4 Å in similar compounds. The Ru–Ru separation of 3.395 (1) Å for **1a** and 3.402 (1) Å for **1b** are well within the range of Ru–Ru distances, 3.28–3.44 Å, reported for the analogous complexes.

Formal oxidation state assignments for the Ru centers were at first ambiguous for compound **1a** since both "$[-Ru^{II}Cl_3Ru^{II}-][Ru^{III}Cl_4L_2]$" and "$[Ru^{III}Cl_3Ru^{II}][Ru^{II}Cl_4L_2]$" were possible. However, no $[Ru^{II}Cl_4L_2]^{2-}$ ion is known and the Ru–Ru separation in the cation is consistent with the II,II assignments. Thus we strongly believed that it was the correct set of formal oxidation states for the Ru atoms. This was confirmed by the preparation and characterization of compound **1b** by simple ion exchange using **1a** and an excess of $NaBPh_4$. Moreover, the EPR

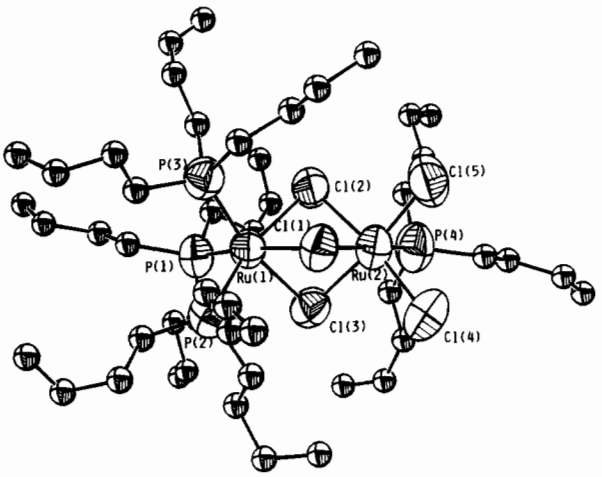

Figure 2. ORTEP drawing of compound **2**. Carbon atoms were given arbitrary radii and were not labeled for clarity.

spectrum of compound **1a** shows an axial pattern ($g_\perp$ = 2.45 and $g_\parallel$ = 1.65), which is almost identical with that previously observed for $[HPEt_3][RuCl_4(PEt_3)_2]$ ($g_\perp$ = 2.51 and $g_\parallel$ = 1.64).[16] Ergo, we assigned the spectrum to the $[Ru^{III}Cl_4(PBu_3)_2]^-$ ion. Compound **1a** has an effective magnetic moment of 2.05 μ_B, which is consistent with the presence of one unpaired electron. This unpaired electron belongs to the Ru(III) monomer. On the other hand, the magnetic susceptibility measurements for compound **1b**, which led to an apparent magnetic moment of 0.71 μ_B/Ru, can be attributed to temperature-independent paramagnetism (TIP). This interpretation is consistent with the result for the $[RuCl_4(PBu_3)_2]^-$ compound. From the g values for this ion we can calculate an expected moment of 1.88 μ_B. If we correct the observed moment of 2.05 μ_B for the contribution from TIP we obtain 1.92 μ_B, which is certainly in agreement within the experimental errors.

Structure and Bonding in the Ru(II), Ru(III) Compounds: $Ru_2Cl_5(PBu_3)_4$ (2). Figure 2 shows the structure of compound 2 while Table XII lists the bond distances and angles of the inner portion of the molecule. The molecule does not have any crystallographically imposed symmetry. However, it has approximate mirror symmetry about the plane containing the two metal atoms and one of the bridging ligands, Cl(1). The Ru–Cl bonds trans to Ru–P bonds, not surprisingly, are longer than those trans to Ru–Cl bonds, and the Ru–Cl_b bond lengths are more than 0.15 Å longer than the terminal Ru–Cl bonds.

The arrangement of the ligands in this green $Ru_2Cl_5(PBu_3)_4$ complex is distinct from that found in the previously characterized brown $Ru_2Cl_5(PBu_3)_4$[9] compound. In the new compound, three PBu_3 ligands are coordinated to one Ru center at the terminal positions while the remaining PBu_3 ligand is similarly ligated to the other Ru center, thus giving the molecule an approximate C_s symmetry. On the other hand, its brown isomeric form has a more symmetric distribution of the PBu_3 ligands; that is, each Ru center has two phosphine ligands cis to each other at the terminal positions. This structure has an approximate C_2 point symmetry. $Ru_2Cl_5(PBu_3)_4$ is the only face-sharing bioctahedral compound of the Ru(II), Ru(III) type proven to exist in two possible structural geometries. The Ru–Ru separation in the C_s isomer is 3.279 (2) Å, identical with that observed for the analogous PEt_2Ph complex.[8] The EPR spectrum showed an axial pattern ($g_\perp$ = 2.44, $g_\parallel$ = 1.59) as seen in Figure 3.

$Ru_2Cl_5(PMe_2Ph)_4$ (3). The structure of this compound is shown in Figure 4, and the bond distances and angles for the core of the molecule are listed in Table XIII. The molecule has a crystallographic 2-fold axis of symmetry that passes along the bridging chlorine ligand, Cl(1), and is perpendicular to the metal–metal

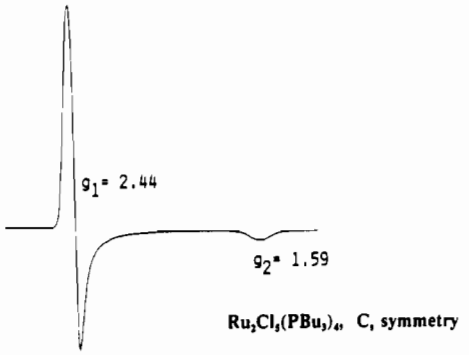

Figure 3. EPR spectrum of a frozen CH_2Cl_2–toluene solution of compound **2** at 77 K.

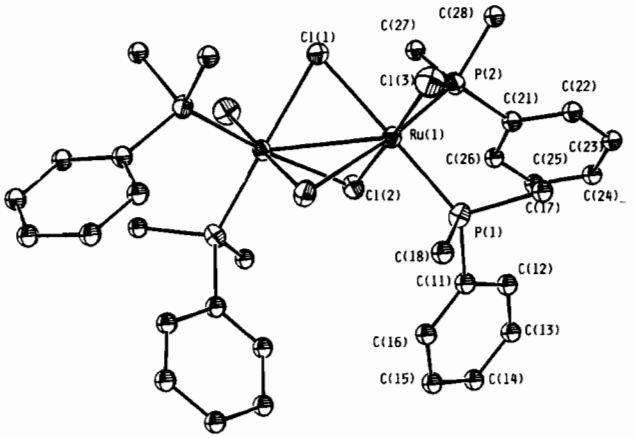

Figure 4. ORTEP drawing of compound **3**. Each unlabeled atom is related to a labeled one by a crystallographic 2-fold axis passing along Cl(1) perpendicular to the Ru–Ru bond. Carbon atoms were given arbitrary radii.

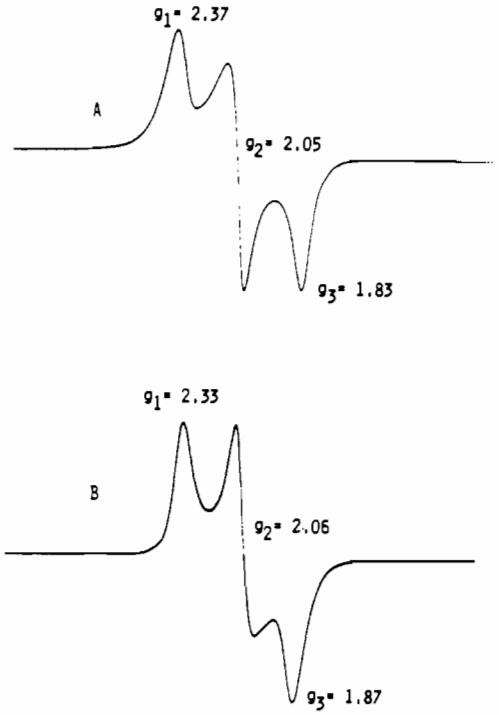

Figure 5. EPR spectra of frozen CH_2Cl_2–toluene solutions of (A) the C_2 isomer of **2**, and (B) compound **3** at 77 K.

vector. This symmetry relates each unlabeled atom to a labeled one. Again, the average of the bridging Ru–Cl bonds is longer than the average of the terminal Ru–Cl bonds by more than 0.15 Å, and the Ru–Cl bonds that are trans to Ru–P bonds are longer

(16) Hudson, A.; Kennedy, M. J. *J. Chem. Soc. A* **1969**, 1116.
(17) Heath, G. A.; Lindsay, A. J.; Stephenson, T. A.; Vattis, D. K. *J. Organomet. Chem.* **1982**, *233*, 353.

Table V. Positional and Isotropic-Equivalent Thermal Displacement Parameters (B_{iso} in Å^2) for $[Ru_2Cl_3(PBu_3)_6][BPh_4]$[a]

atom	x	y	z	B_{iso}	atom	x	y	z	B_{iso}
Ru(1)	0.30989 (2)	0.21430 (5)	0.02414 (2)	3.32 (1)	C(54)	0.3649 (3)	0.7474 (7)	0.3990 (4)	5.1 (2)
Ru(2)	0.22796 (2)	0.75830 (5)	0.44007 (2)	3.27 (1)	C(55)	0.4188 (4)	0.7215 (9)	0.4162 (5)	7.2 (3)
Cl(1)	0.250	0.3474 (2)	0.000	3.64 (6)	C(56)	0.4514 (4)	0.8179 (9)	0.4141 (5)	8.2 (4)
Cl(2)	0.26348 (7)	0.1440 (2)	−0.05123 (7)	4.27 (5)	C(57)	0.2608 (4)	0.7020 (7)	0.3239 (3)	5.3 (3)
Cl(3)	0.250	0.6238 (2)	0.500	3.67 (6)	C(58)	0.2846 (5)	0.6331 (8)	0.2915 (4)	7.3 (3)
Cl(4)	0.19688 (7)	0.8258 (2)	0.51191 (7)	3.79 (5)	C(59)	0.2698 (7)	0.678 (1)	0.2366 (5)	12.3 (6)
P(1)	0.33428 (7)	0.3007 (2)	0.09459 (8)	4.08 (5)	C(60)	0.279 (1)	0.617 (2)	0.2023 (7)	23 (1)
P(2)	0.36922 (7)	0.2788 (2)	−0.01534 (8)	4.02 (5)	C(61)	0.1024 (3)	0.7796 (7)	0.4197 (4)	5.7 (3)
P(3)	0.34908 (8)	0.0687 (2)	0.04675 (8)	4.28 (6)	C(62)	0.0515 (4)	0.746 (1)	0.4097 (7)	12.2 (6)
P(4)	0.22106 (8)	0.9051 (2)	0.39817 (8)	3.95 (5)	C(63)	0.015 (1)	0.823 (2)	0.428 (1)	18 (1)
P(5)	0.26794 (8)	0.6685 (2)	0.38853 (8)	3.92 (5)	C(64)	0.011 (1)	0.897 (2)	0.396 (1)	19 (1)
P(6)	0.15183 (8)	0.6941 (2)	0.41176 (8)	4.18 (5)	C(65)	0.1354 (4)	0.6442 (9)	0.3497 (4)	7.9 (4)
C(1)	0.2877 (3)	0.3096 (8)	0.1336 (3)	5.4 (3)	C(66)	0.1131 (7)	0.693 (1)	0.3108 (5)	14.4 (7)
C(2)	0.2823 (5)	0.239 (1)	0.1680 (5)	11.7 (6)	C(67)	0.0979 (6)	0.639 (1)	0.2641 (5)	11.4 (5)
C(3)	0.2523 (5)	0.291 (2)	0.2086 (5)	12.6 (6)	C(68)	0.0920 (7)	0.707 (2)	0.2234 (7)	14.8 (8)
C(4)	0.2519 (8)	0.216 (3)	0.2459 (8)	24 (1)	C(69)	0.1399 (3)	0.5858 (8)	0.4497 (4)	6.5 (3)
C(5)	0.3889 (3)	0.2599 (8)	0.1346 (3)	5.3 (2)	C(70)	0.0953 (5)	0.521 (1)	0.4329 (6)	11.4 (5)
C(6)	0.4021 (4)	0.311 (1)	0.1851 (4)	10.1 (5)	C(71)	0.0900 (5)	0.448 (1)	0.4774 (8)	12.5 (6)
C(7)	0.4489 (5)	0.258 (2)	0.2110 (4)	12.7 (6)	C(72)	0.0507 (8)	0.410 (2)	0.481 (1)	20 (1)
C(8)	0.453 (1)	0.233 (2)	0.2531 (9)	20 (1)	C(73)	0.5193 (2)	0.3752 (4)	−0.2032 (2)	4.5 (2)
C(9)	0.3490 (4)	0.4338 (7)	0.0874 (4)	6.6 (3)	C(74)	0.5348 (2)	0.3067 (4)	−0.1667 (2)	5.4 (3)
C(10)	0.3095 (5)	0.509 (1)	0.0820 (6)	10.3 (5)	C(75)	0.5376 (2)	0.3346 (4)	−0.1184 (2)	6.5 (3)
C(11)	0.3330 (6)	0.615 (1)	0.080 (1)	14.7 (8)	C(76)	0.5251 (2)	0.4310 (4)	−0.1066 (2)	6.6 (3)
C(12)	0.290 (1)	0.673 (2)	0.062 (1)	21 (1)	C(77)	0.5096 (2)	0.4995 (4)	−0.1431 (2)	6.5 (3)
C(13)	0.3875 (3)	0.2051 (7)	−0.0653 (3)	4.9 (2)	C(78)	0.5067 (2)	0.4716 (4)	−0.1914 (2)	5.9 (3)
C(14)	0.3515 (4)	0.202 (1)	−0.1134 (4)	8.8 (4)	C(79)	0.5406 (2)	0.4327 (5)	−0.2895 (2)	4.9 (2)
C(15)	0.3747 (5)	0.146 (1)	−0.1536 (4)	11.3 (6)	C(80)	0.5863 (2)	0.4670 (5)	−0.2690 (2)	5.9 (3)
C(16)	0.4144 (5)	0.203 (1)	−0.1691 (5)	10.1 (5)	C(81)	0.6109 (2)	0.5358 (5)	−0.2937 (2)	6.8 (3)
C(17)	0.4286 (3)	0.3094 (7)	0.0207 (3)	4.8 (2)	C(82)	0.5898 (2)	0.5702 (5)	−0.3390 (2)	7.4 (4)
C(18)	0.4744 (3)	0.2970 (9)	−0.0027 (4)	6.5 (3)	C(83)	0.5442 (2)	0.5359 (5)	−0.3595 (2)	7.0 (3)
C(19)	0.5196 (3)	0.326 (1)	0.0358 (4)	7.4 (3)	C(84)	0.5196 (2)	0.4671 (5)	−0.3348 (2)	6.0 (3)
C(20)	0.5651 (8)	0.297 (2)	0.0217 (9)	20 (1)	C(85)	0.5411 (2)	0.2349 (4)	−0.2655 (2)	4.9 (2)
C(21)	0.3488 (4)	0.3971 (7)	−0.0461 (4)	6.5 (3)	C(86)	0.5879 (2)	0.2271 (4)	−0.2771 (2)	5.4 (3)
C(22)	0.3877 (4)	0.447 (1)	−0.0725 (5)	8.6 (4)	C(87)	0.6093 (2)	0.1338 (4)	−0.2795 (2)	6.8 (3)
C(23)	0.3532 (9)	0.544 (2)	−0.1016 (8)	16.7 (9)	C(88)	0.5839 (2)	0.0482 (4)	−0.2704 (2)	8.2 (4)
C(24)	0.359 (1)	0.535 (3)	−0.143 (1)	28 (2)	C(89)	0.5370 (2)	0.0560 (4)	−0.2588 (2)	7.9 (4)
C(25)	0.4158 (3)	0.0616 (7)	0.0534 (4)	5.5 (3)	C(90)	0.5156 (2)	0.1493 (4)	−0.2564 (2)	7.5 (4)
C(26)	0.4383 (4)	−0.0427 (8)	0.0679 (5)	7.5 (3)	C(91)	0.4564 (3)	0.3336 (5)	−0.2844 (2)	5.8 (3)
C(27)	0.4962 (4)	−0.027 (1)	0.0788 (5)	9.2 (4)	C(92)	0.4188 (3)	0.3730 (5)	−0.2625 (2)	7.0 (3)
C(28)	0.5079 (5)	0.019 (1)	0.1290 (6)	13.3 (6)	C(93)	0.3708 (3)	0.3624 (5)	−0.2845 (2)	9.4 (5)
C(29)	0.3367 (4)	0.0257 (8)	0.1062 (3)	6.2 (3)	C(94)	0.3604 (3)	0.3124 (5)	−0.3285 (2)	12.1 (6)
C(30)	0.3212 (9)	−0.073 (1)	0.1110 (6)	18 (1)	C(95)	0.3980 (3)	0.2731 (5)	−0.3504 (2)	11.0 (5)
C(31)	0.3111 (8)	−0.104 (1)	0.1647 (5)	13.2 (7)	C(96)	0.4460 (3)	0.2837 (5)	−0.3284 (2)	7.9 (4)
C(32)	0.2864 (7)	−0.034 (2)	0.1914 (7)	13.2 (7)	B	0.5145 (4)	0.3452 (9)	−0.2610 (4)	4.9 (3)
C(33)	0.3297 (3)	−0.0397 (7)	0.0070 (4)	5.2 (2)	H(1)	0.5445 (2)	0.2321 (4)	−0.1759 (2)	5.527*
C(34)	0.3471 (4)	−0.0413 (7)	−0.0414 (4)	5.7 (3)	H(2)	0.5496 (2)	0.2816 (4)	−0.0902 (2)	5.527*
C(35)	0.3270 (4)	−0.1391 (9)	−0.0682 (4)	8.1 (4)	H(3)	0.5273 (2)	0.4526 (4)	−0.0692 (2)	5.527*
C(36)	0.3443 (5)	−0.141 (1)	−0.1197 (5)	10.5 (5)	H(4)	0.4999 (2)	0.5741 (4)	−0.1339 (2)	5.527*
C(37)	0.2068 (3)	1.0145 (6)	0.4331 (3)	4.2 (2)	H(5)	0.4948 (2)	0.5246 (4)	−0.2196 (2)	5.527*
C(38)	0.1532 (3)	1.0224 (7)	0.4421 (3)	5.2 (2)	H(6)	0.6025 (2)	0.4403 (5)	−0.2339 (2)	5.527*
C(39)	0.1485 (4)	1.1147 (8)	0.4747 (4)	6.3 (3)	H(7)	0.6462 (2)	0.5624 (5)	−0.2778 (2)	5.527*
C(40)	0.0953 (5)	1.122 (1)	0.4861 (5)	10.0 (5)	H(8)	0.6089 (2)	0.6235 (5)	−0.3581 (2)	5.527*
C(41)	0.1791 (4)	0.9185 (7)	0.3411 (3)	5.5 (3)	H(9)	0.5279 (2)	0.5626 (5)	−0.3945 (2)	5.527*
C(42)	0.1741 (4)	1.0229 (8)	0.3194 (4)	6.7 (3)	H(10)	0.4843 (2)	0.4405 (5)	−0.3507 (2)	5.527*
C(43)	0.1371 (7)	1.024 (1)	0.2737 (7)	14.2 (7)	H(11)	0.6076 (2)	0.2934 (4)	−0.2842 (2)	5.527*
C(44)	0.0978 (8)	0.991 (2)	0.272 (1)	21 (1)	H(12)	0.6456 (2)	0.1278 (4)	−0.2885 (2)	5.527*
C(45)	0.2798 (4)	0.9432 (8)	0.3797 (4)	6.4 (3)	H(13)	0.6004 (2)	−0.0240 (4)	−0.2722 (2)	5.527*
C(46)	0.2949 (4)	1.0455 (8)	0.3756 (6)	9.6 (5)	H(14)	0.5173 (2)	−0.0103 (4)	−0.2517 (2)	5.527*
C(47)	0.3462 (4)	1.0620 (8)	0.3628 (5)	7.3 (4)	H(15)	0.4794 (2)	0.1553 (4)	−0.2474 (2)	5.527*
C(48)	0.3610 (6)	1.160 (1)	0.3581 (8)	13.8 (7)	H(16)	0.4268 (3)	0.4117 (5)	−0.2285 (2)	5.527*
C(49)	0.2486 (3)	0.5343 (6)	0.3870 (4)	5.4 (3)	H(17)	0.3417 (3)	0.3928 (5)	−0.2676 (2)	5.527*
C(50)	0.2872 (6)	0.4584 (9)	0.4075 (7)	13.0 (7)	H(18)	0.3233 (3)	0.3042 (5)	−0.3456 (2)	5.527*
C(51)	0.2623 (7)	0.354 (1)	0.4133 (9)	15.3 (8)	H(19)	0.3900 (3)	0.2344 (5)	−0.3845 (2)	5.527*
C(52)	0.293 (1)	0.296 (2)	0.4442 (9)	25 (2)	H(20)	0.4751 (3)	0.2532 (5)	−0.3454 (2)	5.527*
C(53)	0.3348 (3)	0.6570 (7)	0.4064 (3)	5.0 (2)					

[a] Values for anisotropically refined atoms are given in the form of the equivalent isotropic displacement parameter defined as $(4/3)[a^2B_{11} + b^2B_{22} + c^2B_{33} + ab(\cos\gamma)B_{12} + ac(\cos\beta)B_{13} + bc(\cos\alpha)B_{23}]$. Starred values denote atoms in calculated positions that were not refined. The numbers in parentheses are the estimated standard deviations in the least significant digit.

than those trans to Ru–Cl bonds.

The ligand arrangement and the 2-fold symmetry along Cl(1) is identical with that of the C_2 isomer[9] of compound **2**. However, the Ru–Ru separation of 2.9941 (4) Å is significantly shorter in this case. The effective magnetic moment of 1.94 μ_B/molecule is consistent with the presence of one unpaired electron. The EPR spectra for both compound **3** and the isomer of compound **2** having C_2 symmetry are shown in Figure 5.

$Ru_2Cl_5(PMe_3)_4$ (4). There is no crystallographic symmetry contained in this molecule, but there is approximate mirror symmetry about a plane defined by the two ruthenium atoms and the bridging chlorine ligand, Cl(1), trans to the terminal chlorine atoms, Cl(4) and Cl(5). There is also a second approximate mirror plane defined by Cl(1), Cl(2), and Cl(3), the three bridging

Table VI. Positional and Isotropic-Equivalent Thermal Displacement Parameters (B_{iso} in Å^2) for $Ru_2Cl_5(PBu_3)_4$[a]

atom	x	y	z	B_{iso}
Ru(1)	0.46595 (7)	0.0495 (1)	0.21900 (6)	7.38 (5)
Ru(2)	0.63519 (8)	0.0428 (1)	0.27597 (6)	9.17 (6)
Cl(1)	0.5736 (2)	0.1004 (4)	0.1862 (2)	9.0 (2)
Cl(2)	0.5497 (2)	−0.0895 (3)	0.2569 (2)	8.7 (2)
Cl(3)	0.5352 (2)	0.1245 (4)	0.3025 (2)	8.8 (2)
Cl(4)	0.7023 (3)	0.1879 (4)	0.2879 (2)	12.4 (2)
Cl(5)	0.7203 (3)	−0.0461 (5)	0.2422 (2)	12.4 (2)
P(1)	0.3765 (3)	0.0081 (4)	0.2641 (2)	8.4 (2)
P(2)	0.4203 (3)	0.1984 (4)	0.1847 (2)	9.3 (2)
P(3)	0.4238 (3)	−0.0452 (4)	0.1450 (2)	8.9 (2)
P(4)	0.6832 (3)	−0.0118 (5)	0.3591 (2)	11.4 (2)
C(1)	0.390 (1)	−0.115 (2)	0.301 (1)	13 (1)
C(2)	0.441 (2)	−0.097 (2)	0.348 (1)	14 (1)
C(3)	0.460 (2)	−0.186 (3)	0.383 (2)	31 (3)
C(4)	0.449 (3)	−0.276 (3)	0.364 (2)	24 (2)
C(5)	0.364 (1)	0.104 (2)	0.3147 (9)	9.2 (8)
C(6)	0.315 (2)	0.074 (2)	0.349 (1)	13 (1)
C(7)	0.322 (2)	0.152 (2)	0.392 (1)	15 (1)
C(8)	0.296 (3)	0.133 (3)	0.434 (1)	28 (3)
C(9)	0.285 (1)	−0.006 (2)	0.2218 (8)	10.3 (8)
C(10)	0.232 (1)	−0.060 (3)	0.242 (1)	21 (2)
C(11)	0.164 (2)	−0.059 (4)	0.196 (2)	26 (2)
C(12)	0.123 (2)	−0.123 (6)	0.209 (2)	48 (5)
C(13)	0.324 (1)	0.230 (2)	0.1767 (9)	11.0 (8)
C(14)	0.305 (2)	0.328 (2)	0.145 (1)	16 (1)
C(15)	0.227 (2)	0.342 (3)	0.135 (1)	18 (2)
C(16)	0.193 (2)	0.296 (4)	0.092 (1)	24 (2)
C(17)	0.436 (1)	0.210 (2)	0.114 (1)	12 (1)
C(18)	0.471 (2)	0.298 (3)	0.103 (1)	16 (1)
C(19)	0.482 (2)	0.294 (3)	0.048 (2)	20 (2)
C(20)	0.521 (3)	0.362 (4)	0.028 (2)	27 (2)
C(21)	0.469 (1)	0.307 (2)	0.216 (1)	12 (1)
C(22)	0.434 (2)	0.328 (2)	0.264 (1)	17 (2)
C(23)	0.467 (2)	0.425 (4)	0.288 (2)	28 (3)
C(24)	0.539 (2)	0.414 (2)	0.316 (2)	22 (2)
C(25)	0.340 (1)	−0.006 (2)	0.1030 (9)	10.4 (8)
C(26)	0.327 (2)	−0.035 (3)	0.051 (1)	22 (2)
C(27)	0.258 (2)	0.013 (4)	0.017 (1)	23 (2)
C(28)	0.200 (2)	−0.042 (4)	0.020 (2)	27 (3)
C(29)	0.408 (1)	−0.180 (2)	0.1635 (8)	9.7 (8)
C(30)	0.387 (1)	−0.250 (2)	0.118 (1)	13 (1)
C(31)	0.374 (2)	−0.347 (3)	0.142 (2)	21 (2)
C(32)	0.418 (3)	−0.402 (3)	0.157 (3)	30 (3)
C(33)	0.487 (1)	−0.057 (2)	0.0962 (7)	8.7 (7)
C(34)	0.554 (1)	−0.123 (2)	0.1181 (9)	9.9 (8)
C(35)	0.598 (1)	−0.112 (2)	0.074 (1)	14 (1)
C(36)	0.663 (2)	−0.177 (2)	0.090 (1)	18 (1)
C(37)	0.782 (1)	0.015 (2)	0.379 (1)	14 (1)
C(38)	0.812 (2)	−0.013 (3)	0.434 (1)	20 (2)
C(39)	0.891 (2)	0.037 (6)	0.440 (2)	30 (3)
C(40)	0.917 (3)	0.042 (7)	0.492 (2)	49 (5)
C(41)	0.636 (2)	0.032 (3)	0.414 (1)	16 (1)
C(42)	0.653 (2)	0.136 (3)	0.420 (1)	16 (1)
C(43)	0.615 (2)	0.189 (4)	0.460 (2)	40 (4)
C(44)	0.552 (2)	0.190 (5)	0.456 (2)	38 (4)
C(45)	0.672 (1)	−0.140 (2)	0.367 (1)	14 (1)
C(46)	0.702 (2)	−0.213 (3)	0.370 (2)	27 (3)
C(47)	0.685 (3)	−0.323 (3)	0.375 (2)	22 (2)
C(48)	0.711 (4)	−0.360 (4)	0.422 (2)	31 (3)

[a] Values for anisotropically refined atoms are given in the form of the equivalent isotropic displacement parameter defined as: $(4/3)[a^2B_{11} + b^2B_{22} + c^2B_{33} + ab(\cos\gamma)B_{12} + ac(\cos\beta)B_{13} + bc(\cos\alpha)B_{23}]$. The numbers in parentheses are the estimated standard deviations in the least significant digit.

Table VII. Positional and Isotropic-Equivalent Thermal Displacement Parameters (B_{iso} in Å^2) for $Ru_2Cl_5(PMe_2Ph)_4$[a]

atom	x	y	z	B_{iso}
Ru(1)	0.45801 (2)	0.01178 (3)	0.68047 (2)	1.476 (6)
Cl(1)	0.500	0.1876 (1)	0.750	2.03 (3)
Cl(2)	0.40201 (6)	−0.0783 (1)	0.76514 (5)	1.99 (2)
Cl(3)	0.51783 (7)	0.1020 (1)	0.59948 (6)	2.65 (2)
P(1)	0.43776 (7)	−0.1484 (1)	0.61124 (5)	1.85 (2)
P(2)	0.32829 (7)	0.1073 (1)	0.64636 (5)	1.81 (2)
C(11)	0.3859 (3)	−0.2819 (4)	0.6335 (2)	1.97 (9)
C(12)	0.2977 (3)	−0.2983 (4)	0.6141 (3)	2.7 (1)
C(13)	0.2569 (3)	−0.3987 (5)	0.6304 (3)	3.1 (1)
C(14)	0.3043 (4)	−0.4861 (5)	0.6666 (3)	3.4 (1)
C(15)	0.3922 (4)	−0.4738 (5)	0.6857 (3)	4.5 (1)
C(16)	0.4321 (3)	−0.3707 (5)	0.6703 (3)	3.6 (1)
C(17)	0.3779 (3)	−0.1175 (5)	0.5304 (2)	2.8 (1)
C(18)	0.5396 (3)	−0.2063 (5)	0.5944 (3)	3.0 (1)
C(21)	0.2307 (3)	0.0223 (4)	0.6134 (2)	2.09 (9)
C(22)	0.1900 (3)	0.0285 (4)	0.5489 (2)	2.6 (1)
C(23)	0.1146 (3)	−0.0364 (5)	0.5269 (2)	3.0 (1)
C(24)	0.0789 (3)	−0.1035 (5)	0.5682 (3)	3.1 (1)
C(25)	0.1190 (3)	−0.1115 (5)	0.6324 (3)	3.0 (1)
C(26)	0.1944 (3)	−0.0480 (5)	0.6552 (2)	2.6 (1)
C(27)	0.2919 (3)	0.1880 (4)	0.7104 (2)	2.5 (1)
C(28)	0.3287 (3)	0.2245 (5)	0.5870 (3)	2.8 (1)
H(1)	0.329 (3)	−0.084 (5)	0.531 (2)	1.2 (4)*
H(2)	0.377 (3)	−0.185 (5)	0.502 (2)	1.2*
H(3)	0.405 (3)	−0.058 (5)	0.513 (2)	1.2*
H(4)	0.573 (3)	−0.227 (5)	0.633 (3)	1.2*
H(5)	0.565 (3)	−0.148 (5)	0.578 (2)	1.2*
H(6)	0.524 (3)	−0.262 (5)	0.561 (3)	1.2*
H(7)	0.270 (3)	−0.233 (4)	0.590 (2)	0.6 (3)*
H(8)	0.207 (3)	−0.410 (5)	0.618 (2)	0.6*
H(9)	0.279 (3)	−0.556 (5)	0.678 (2)	0.6*
H(10)	0.485 (3)	−0.356 (4)	0.685 (2)	0.6*
H(11)	0.426 (3)	−0.533 (4)	0.714 (2)	0.6*
H(12)	0.288 (3)	0.136 (5)	0.740 (2)	1.2*
H(13)	0.324 (3)	0.241 (5)	0.728 (3)	1.2*
H(14)	0.226 (3)	0.230 (5)	0.698 (3)	1.2*
H(15)	0.332 (3)	0.191 (5)	0.555 (2)	1.2*
H(16)	0.376 (3)	0.276 (5)	0.602 (2)	1.2*
H(17)	0.262 (3)	0.271 (5)	0.577 (3)	1.2*
H(18)	0.209 (3)	0.081 (4)	0.522 (2)	0.6*
H(19)	0.085 (3)	−0.032 (5)	0.486 (2)	0.6*
H(20)	0.027 (3)	−0.146 (5)	0.552 (2)	0.6*
H(21)	0.099 (3)	−0.161 (4)	0.664 (2)	0.6*
H(22)	0.226 (3)	−0.053 (5)	0.697 (2)	0.6*

[a] Values for anisotropically refined atoms are given in the form of the equivalent isotropic displacement parameter defined as: $(4/3)[a^2B_{11} + b^2B_{22} + c^2B_{33} + ab(\cos\gamma)B_{12} + ac(\cos\beta)B_{13} + bc(\cos\alpha)B_{23}]$. Starred values denote atoms that were refined isotropically. The numbers in parentheses are the estimated standard deviations in the least significant light.

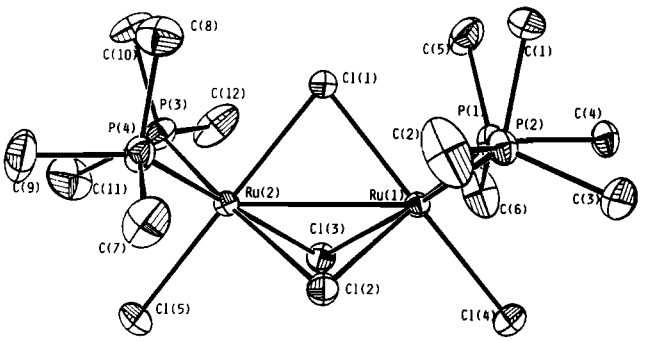

Figure 6. ORTEP drawing of compound **4**. Carbon atoms were given arbitrary radii.

chlorine atoms. These give the molecule C_{2v} point group symmetry. This structure, shown in Figure 6, is the first face-sharing bioctahedron of the type studied here with this symmetry to be structurally characterized. The other possible isomers, those having C_s or C_2 symmetry, have been discussed earlier for similar face-sharing bioctahedra. Compound **2** displays C_s symmetry and compound **3** displays C_2 symmetry.

The pertinent bond distances and angles for compound **4** are listed in Table XIV. The shortest Ru–Cl_b distance, 2.385 (2) Å, is longer than both terminal Ru–Cl bonds, 2.351 (2) and 2.348 (2) Å, as expected. As is typically the case, the Ru–Cl bonds trans to Ru–P bonds are longer than those trans to Ru–Cl bonds. The Ru–Ru separation of 2.992 (1) Å is essentially the same as that in compound **3**. EPR experiments gave rhombic spectral patterns (g_1 = 2.29, g_2 = 2.07, g_3 = 1.90).

Table VIII. Positional and Isotropic-Equivalent Thermal Displacement Parameters (B_{iso} in Å^2) for $Ru_2Cl_5(PMe_3)_4$[a]

atom	x	y	z	B_{iso}
Ru(1)	0.23253 (5)	0.584 (0)	0.41933 (4)	1.305 (7)
Ru(2)	0.27039 (5)	0.48414 (5)	0.17781 (4)	1.365 (8)
Cl(1)	0.1846 (2)	0.6562 (1)	0.2190 (1)	1.68 (3)
Cl(2)	0.1349 (2)	0.4155 (1)	0.3431 (1)	1.92 (3)
Cl(3)	0.4598 (2)	0.5123 (1)	0.3507 (2)	1.83 (3)
Cl(4)	0.2868 (2)	0.5148 (2)	0.6166 (2)	2.24 (3)
Cl(5)	0.3515 (2)	0.3137 (2)	0.1417 (2)	2.85 (4)
P(1)	0.3501 (2)	0.7339 (2)	0.4930 (2)	1.84 (3)
P(2)	0.0060 (2)	0.6383 (2)	0.4612 (2)	1.73 (3)
P(3)	0.4177 (2)	0.5563 (2)	0.0437 (2)	2.06 (3)
P(4)	0.0798 (2)	0.4523 (2)	0.0357 (2)	1.96 (3)
C(1)	−0.0484 (9)	0.7702 (7)	0.4131 (7)	2.7 (1)
C(2)	−0.1413 (9)	0.5641 (9)	0.380 (1)	4.3 (2)
C(3)	−0.0397 (9)	0.6323 (8)	0.6198 (7)	3.0 (2)
C(4)	0.2911 (8)	0.7889 (6)	0.6347 (6)	2.1 (1)
C(5)	0.346 (1)	0.8477 (7)	0.3896 (7)	3.1 (2)
C(6)	0.5435 (9)	0.7142 (9)	0.5384 (9)	3.9 (2)
C(7)	−0.051 (1)	0.3604 (8)	0.0871 (8)	3.5 (2)
C(8)	−0.0373 (8)	0.5607 (7)	−0.0139 (8)	2.9 (2)
C(9)	0.118 (1)	0.3930 (9)	−0.1076 (8)	3.7 (2)
C(10)	0.3346 (8)	0.6476 (7)	−0.0706 (7)	2.7 (1)
C(11)	0.514 (1)	0.4662 (9)	−0.0494 (9)	4.6 (2)
C(12)	0.566 (1)	0.6342 (9)	0.1158 (8)	3.9 (2)

[a] Values for anisotropically refined atoms are given in the form of the equivalent isotropic displacement parameter defined as: $(4/3)[a^2B_{11} + b^2B_{22} + c^2B_{33} + ab(\cos\gamma)B_{12} + ac(\cos\beta)B_{13} + bc(\cos\alpha)B_{23}]$. The numbers in parentheses are the estimated standard deviations in the least significant digit.

Table IX. Positional and Isotropic-Equivalent Thermal Displacement Parameters (B_{iso} in Å^2) for $Ru_2Cl_6(PEt_3)_3$[a]

atom	x	y	z	B_{iso}
Ru(1)	0.64429 (6)	0.74606 (4)	0.06380 (8)	2.12 (1)
Ru(2)	0.36645 (6)	0.75212 (4)	0.13840 (8)	2.24 (1)
Cl(1)	0.4858 (2)	0.7479 (1)	−0.1351 (2)	2.66 (4)
Cl(2)	0.4967 (2)	0.6564 (1)	0.2099 (3)	2.98 (4)
Cl(3)	0.5369 (2)	0.8404 (1)	0.2391 (3)	2.93 (4)
Cl(4)	0.7920 (2)	0.7434 (1)	0.2711 (3)	3.59 (5)
Cl(5)	0.2615 (2)	0.8507 (1)	0.0478 (3)	3.67 (5)
Cl(6)	0.2218 (2)	0.6584 (1)	0.0205 (3)	3.84 (5)
P(1)	0.7234 (2)	0.6428 (1)	−0.0799 (3)	2.49 (4)
P(2)	0.7513 (2)	0.8450 (1)	−0.0725 (3)	2.75 (4)
P(3)	0.2757 (2)	0.7542 (1)	0.3901 (3)	2.62 (4)
C(1)	0.6959 (9)	0.5498 (5)	0.018 (1)	4.0 (2)
C(2)	0.763 (1)	0.5452 (7)	0.190 (1)	6.3 (3)
C(3)	0.8859 (8)	0.6552 (5)	−0.104 (1)	3.6 (2)
C(4)	0.9377 (9)	0.5817 (6)	−0.187 (2)	5.3 (3)
C(5)	0.6571 (8)	0.6183 (5)	−0.297 (1)	3.5 (2)
C(6)	0.5376 (9)	0.5683 (6)	−0.306 (1)	4.8 (2)
C(7)	0.7533 (9)	0.8274 (5)	−0.304 (1)	3.6 (2)
C(8)	0.809 (1)	0.8970 (6)	−0.396 (1)	4.9 (2)
C(9)	0.6905 (9)	0.9395 (5)	−0.048 (1)	3.8 (2)
C(10)	0.573 (1)	0.9438 (6)	−0.149 (1)	4.5 (2)
C(11)	0.9131 (8)	0.8676 (7)	−0.006 (1)	4.6 (2)
C(12)	0.938 (1)	0.9247 (7)	0.153 (1)	5.5 (3)
C(13)	0.3351 (9)	0.8344 (5)	0.544 (1)	3.8 (2)
C(14)	0.311 (1)	0.9157 (6)	0.498 (2)	5.8 (3)
C(15)	0.2961 (9)	0.6699 (5)	0.514 (1)	3.4 (2)
C(16)	0.232 (1)	0.5928 (6)	0.434 (1)	4.4 (2)
C(17)	0.1122 (8)	0.7579 (7)	0.369 (1)	4.5 (2)
C(18)	0.0525 (9)	0.7605 (9)	0.545 (1)	6.2 (3)

[a] Values for anisotropically refined atoms are given in the form of the equivalent isotropic displacement parameter defined as: $(4/3)[a^2B_{11} + b^2B_{22} + c^2B_{33} + ab(\cos\gamma)B_{12} + ac(\cos\beta)B_{13} + bc(\cos\alpha)B_{23}]$. The numbers in parentheses are the estimated standard deviations in the least significant digit.

Structure and Bonding in the Ru(III), Ru(III) Compounds: $Ru_2Cl_6(PEt_3)_3$ (5). The structure of compound **5** is shown in Figure 7, and important bond distances and angles are listed in Table XV. There is no crystallographically imposed symmetry in the molecule, but the inner portion, i.e., excluding the ethyl groups, possess approximate mirror symmetry about the plane

Table X. Selected Bond Distances (Å) and Angles (deg) for $[Ru_2Cl_3(PBu_3)_6][RuCl_4(PBu_3)_2]$[a]

Bond Distances			
Ru(1)–Cl(1)	2.495 (2)	Ru(1)–P(3)	2.289 (2)
Ru(1)–Cl(2)	2.486 (2)	Ru(2)–Cl(3)	2.360 (3)
Ru(1)–Cl(2′)	2.473 (2)	Ru(2)–Cl(4)	2.370 (3)
Ru(1)–P(1)	2.308 (2)	Ru(2)–P(4)	2.375 (3)
Ru(1)–P(2)	2.292 (3)		
Bond Angles			
Cl(1)–Ru(1)–Cl(2)	77.74 (6)	P(1)–Ru(1)–P(3)	95.49 (9)
Cl(1)–Ru(1)–Cl(2′)	77.97 (6)	P(2)–Ru(1)–P(3)	96.46 (9)
Cl(1)–Ru(1)–P(1)	166.78 (8)	Cl(3)–Ru(2)–Cl(3′)	180.00 (0)
Cl(1)–Ru(1)–P(2)	89.82 (7)	Cl(3)–Ru(2)–Cl(4)	90.36 (9)
Cl(1)–Ru(1)–P(3)	95.69 (7)	Cl(3′)–Ru(2)–Cl(4)	89.64 (9)
Cl(2)–Ru(1)–Cl(2′)	79.65 (8)	Cl(3)–Ru(2)–P(4)	91.01 (9)
Cl(2)–Ru(1)–P(1)	96.13 (9)	Cl(3′)–Ru(2)–P(4)	88.99 (9)
Cl(2)–Ru(1)–P(2)	167.54 (8)	Cl(4)–Ru(2)–Cl(4′)	180.00 (0)
Cl(2)–Ru(1)–P(3)	85.56 (9)	Cl(4)–Ru(2)–P(4)	89.06 (9)
Cl(2′)–Ru(1)–P(1)	89.46 (8)	Cl(4′)–Ru(2)–P(4)	90.94 (9)
Cl(2′)–Ru(1)–P(2)	97.28 (8)	P(4)–Ru(2)–P(4′)	180.00 (0)
Cl(2′)–Ru(1)–P(3)	164.83 (9)	Ru(1)–Cl(1)–Ru(1′)	85.7 (1)
P(1)–Ru(1)–P(2)	95.92 (9)	Ru(1)–Cl(2)–Ru(1′)	86.39 (8)

[a] Numbers in parentheses are estimated standard deviations in the least significant digits.

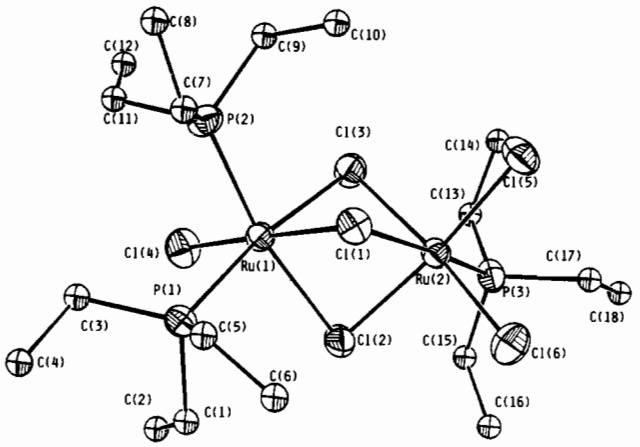

Figure 7. ORTEP drawing of compound **5**. Carbon atoms were given arbitrary radii.

defined by the Ru atoms and the bridging chlorine atom Cl(1). As expected, the Ru–Cl bonds trans to the Ru–P bonds are longer than those trans to the Ru–Cl bonds, and the terminal Ru–Cl bond lengths (average 2.307 (2) Å) are shorter than the bridging Ru–Cl bond distances (average 2.462 (2) Å).

The Ru–Ru distance of 3.201 (1) Å is only slightly longer than that reported for the PBu_3 analogue, 3.176 (1) Å,[1] the only other structurally characterized face-sharing bioctahedral complex of the Ru(III), Ru(III) type with phosphine and chlorine ligands. The magnetic susceptibility measurements gave the following results: $\chi_{mol} = 3.059 \times 10^{-3}$ cgsu, $\mu_{eff} = 2.72\ \mu_B$/molecule. This corresponds to a $\mu_{eff} = 1.91\ \mu_B$/Ru atom, which is consistent with two independent low-spin d^5 configurations.

Cyclic Voltammetric Studies. Results of the cyclic voltammetric studies (including EPR and magnetic susceptibility measurements) for compounds **1a**, **2**, **3**, **4**, and **5** are summarized in Table XVI together with those for previously studied analogous diruthenium complexes. Cyclic voltammograms are shown in Figures 8 and 9. For **1a**, the cyclic voltammogram showed two reversible one-electron-oxidation processes at +1.39 and +0.90 V. The values of the redox potentials are close to that for the one-electron oxidation of the Ru(II) center in compound **2**.

For **2**, a one-electron oxidation is observed at +0.95 V and a one-electron reduction at −0.73 V. The analogous PEt_2Ph compound gave corresponding redox potentials of +1.27 and −0.28 V.[8]

For **3**, the cyclic voltammogram showed a one-electron oxidation at +0.55 V and a one-electron reduction at −0.09 V. The pre-

Table XI. Selected Bond Distances (Å) and Angles (deg) for $[Ru_2Cl_3(PBu_3)_6][BPh_4]$[a]

Bond Distances			
Ru(1)–Cl(1)	2.473 (2)	P(2)–C(13)	1.847 (9)
Ru(1)–Cl(2)	2.494 (2)	P(2)–C(17)	1.854 (8)
Ru(1)–Cl(2)	2.472 (2)	P(2)–C(21)	1.859 (10)
Ru(1)–P(1)	2.304 (2)	P(3)–C(25)	1.845 (8)
Ru(1)–P(2)	2.291 (2)	P(3)–C(29)	1.844 (10)
Ru(1)–P(3)	2.286 (2)	P(3)–C(33)	1.864 (9)
Ru(2)–Cl(3)	2.482 (2)	P(4)–C(37)	1.842 (9)
Ru(2)–Cl(4)	2.478 (2)	P(4)–C(41)	1.844 (9)
Ru(2)–Cl(4)	2.488 (2)	P(4)–C(45)	1.860 (11)
Ru(2)–P(4)	2.290 (2)	P(5)–C(49)	1.882 (9)
Ru(2)–P(5)	2.293 (2)	P(5)–C(53)	1.862 (8)
Ru(2)–P(6)	2.320 (2)	P(5)–C(57)	1.846 (8)
P(1)–C(1)	1.820 (10)	P(6)–C(61)	1.834 (10)
P(1)–C(5)	1.837 (8)	P(6)–C(65)	1.855 (10)
P(1)–C(9)	1.854 (10)	P(6)–C(69)	1.861 (11)

Bond Angles			
Cl(1)–Ru(1)–Cl(2)	78.35 (6)	Ru(1)–P(1)–C(5)	119.0 (3)
Cl(1)–Ru(1)–Cl(2)	78.76 (6)	Ru(1)–P(1)–C(9)	115.8 (4)
Cl(1)–Ru(1)–P(1)	88.35 (7)	C(1)–P(1)–C(5)	104.7 (4)
Cl(1)–Ru(1)–P(2)	95.76 (6)	C(1)–P(1)–C(9)	101.0 (5)
Cl(1)–Ru(1)–P(3)	166.32 (8)	C(5)–P(1)–C(9)	100.3 (5)
Cl(2)–Ru(1)–Cl(2)	76.44 (7)	Ru(1)–P(2)–C(13)	117.5 (3)
Cl(2)–Ru(1)–P(1)	165.20 (7)	Ru(1)–P(2)–C(17)	118.2 (3)
Cl(2)–Ru(1)–P(2)	93.21 (7)	Ru(1)–P(2)–C(21)	110.8 (4)
Cl(2)–Ru(1)–P(3)	94.40 (8)	C(13)–P(2)–C(17)	102.0 (4)
Cl(2)–Ru(1)–P(1)	94.74 (7)	C(13)–P(2)–C(21)	101.9 (5)
Cl(2)–Ru(1)–P(2)	169.03 (7)	C(17)–P(2)–C(21)	104.5 (4)
Cl(2)–Ru(1)–P(3)	88.31 (8)	Ru(1)–P(3)–C(25)	120.4 (3)
P(1)–Ru(1)–P(2)	94.59 (8)	Ru(1)–P(3)–C(29)	111.9 (4)
P(1)–Ru(1)–P(3)	97.24 (8)	Ru(1)–P(3)–C(33)	114.8 (3)
P(2)–Ru(1)–P(3)	96.22 (8)	C(25)–P(3)–C(29)	102.3 (5)
Cl(3)–Ru(2)–Cl(4)	78.40 (6)	C(25)–P(3)–C(33)	102.7 (4)
Cl(3)–Ru(2)–Cl(4)	78.21 (6)	C(29)–P(3)–C(33)	102.6 (5)
Cl(3)–Ru(2)–P(4)	165.53 (7)	Ru(2)–P(4)–C(37)	115.1 (3)
Cl(3)–Ru(2)–P(5)	86.98 (7)	Ru(2)–P(4)–C(41)	121.5 (3)
Cl(3)–Ru(2)–P(6)	94.73 (7)	Ru(2)–P(4)–C(45)	111.7 (3)
Cl(4)–Ru(2)–Cl(4)	78.16 (7)	C(37)–P(4)–C(41)	102.9 (4)
Cl(4)–Ru(2)–P(4)	95.02 (8)	C(37)–P(4)–C(45)	101.3 (4)
Cl(4)–Ru(2)–P(5)	164.77 (7)	C(41)–P(4)–C(45)	101.8 (5)
Cl(4)–Ru(2)–P(6)	90.12 (8)	Ru(2)–P(5)–C(49)	110.8 (3)
Cl(4)–Ru(2)–P(4)	87.88 (7)	Ru(2)–P(5)–C(53)	115.7 (3)
Cl(4)–Ru(2)–P(5)	94.80 (7)	Ru(2)–P(5)–C(57)	119.7 (3)
Cl(4)–Ru(2)–P(6)	167.27 (8)	C(49)–P(5)–C(53)	101.5 (4)
P(4)–Ru(2)–P(5)	98.22 (8)	C(49)–P(5)–C(57)	102.8 (4)
P(4)–Ru(2)–P(6)	98.19 (8)	C(53)–P(5)–C(57)	104.1 (5)
P(5)–Ru(2)–P(6)	95.38 (8)	Ru(2)–P(6)–C(61)	113.0 (3)
Ru(1)–Cl(1)–Ru(1)	87.25 (9)	Ru(2)–P(6)–C(65)	122.8 (4)
Ru(1)–Cl(2)–Ru(1)	86.81 (7)	Ru(2)–P(6)–C(69)	109.1 (3)
Ru(2)–Cl(3)–Ru(2)	86.46 (9)	C(61)–P(6)–C(65)	104.7 (5)
Ru(2)–Cl(4)–Ru(2)	86.44 (7)	C(61)–P(6)–C(69)	102.7 (5)
Ru(1)–P(1)–C(1)	113.7 (3)	C(65)–P(6)–C(69)	102.2 (5)

[a] Numbers in parentheses are estimated standard deviations in the least significant digits.

viously characterized $Ru_2Cl_5(PBu_3)_4$,[9] which has the same approximate symmetry as compound **3**, was also studied and it showed a one-electron oxidation at +0.61 V and a one-electron reduction at −0.28 V. These are the first electrochemical data on $Ru_2Cl_5L_4$ (L = phosphine or arsine) types of compounds having C_2 symmetry that have corresponding x-ray crystal structures. The separation between the redox couples is not as large as those found for the corresponding C_s isomers of these complexes.

The cyclic voltammogram of **4** gave a one-electron oxidation at +0.58 V and a one-electron reduction at −0.18 V. The redox potentials are separated by as much as in those for the diruthenium complexes with the C_2 structure.

Discussion

Structural Results and Their Implications. Table XVII lists all of the chloro–phosphino FSBO complexes of ruthenium for which structural data are available and gives key parameters bearing on the question of whether Ru–Ru bonding occurs.

The five II,II compounds in which no Ru–Ru bonding can be expected because of their d^6,d^6 configurations provide a calibration

Table XII. Selected Bond Distances (Å) and Angles (deg) for $Ru_2Cl_5(PBu_3)_4$[a]

Bond Distances			
Ru(1)–Cl(1)	2.449 (5)	Ru(2)–Cl(1)	2.492 (5)
Ru(1)–Cl(2)	2.524 (5)	Ru(2)–Cl(2)	2.394 (5)
Ru(1)–Cl(3)	2.498 (4)	Ru(2)–Cl(3)	2.400 (5)
Ru(1)–P(1)	2.293 (6)	Ru(2)–Cl(4)	2.315 (6)
Ru(1)–P(2)	2.285 (6)	Ru(2)–Cl(5)	2.303 (6)
Ru(1)–P(3)	2.291 (5)	Ru(2)–P(4)	2.269 (6)

Bond Angles			
Cl(1)–Ru(1)–Cl(2)	80.0 (2)	Cl(1)–Ru(2)–Cl(4)	90.8 (2)
Cl(1)–Ru(1)–Cl(3)	80.6 (2)	Cl(1)–Ru(2)–Cl(5)	93.4 (2)
Cl(1)–Ru(1)–P(1)	170.0 (2)	Cl(1)–Ru(2)–P(4)	175.8 (2)
Cl(1)–Ru(1)–P(2)	84.8 (2)	Cl(2)–Ru(2)–Cl(3)	81.4 (2)
Cl(1)–Ru(1)–P(3)	93.5 (2)	Cl(2)–Ru(2)–Cl(4)	170.4 (2)
Cl(2)–Ru(1)–Cl(3)	77.0 (2)	Cl(2)–Ru(2)–Cl(5)	92.2 (2)
Cl(2)–Ru(1)–P(1)	96.0 (2)	Cl(2)–Ru(2)–P(4)	95.2 (2)
Cl(2)–Ru(1)–P(2)	163.6 (2)	Cl(3)–Ru(2)–Cl(4)	91.5 (2)
Cl(2)–Ru(1)–P(3)	90.3 (2)	Cl(3)–Ru(2)–Cl(5)	172.5 (2)
Cl(3)–Ru(1)–P(1)	89.6 (2)	Cl(3)–Ru(2)–P(4)	94.9 (2)
Cl(3)–Ru(1)–P(2)	94.4 (2)	Cl(4)–Ru(2)–Cl(5)	94.3 (2)
Cl(3)–Ru(1)–P(3)	166.7 (2)	Cl(4)–Ru(2)–P(4)	91.9 (2)
P(1)–Ru(1)–P(2)	97.9 (2)	Cl(5)–Ru(2)–P(4)	89.7 (2)
P(1)–Ru(1)–P(3)	95.8 (2)	Ru(1)–Cl(1)–Ru(2)	83.2 (2)
P(2)–Ru(1)–P(3)	96.9 (2)	Ru(1)–Cl(2)–Ru(2)	83.6 (2)
Cl(1)–Ru(2)–Cl(2)	81.8 (2)	Ru(1)–Cl(3)–Ru(2)	84.0 (2)
Cl(1)–Ru(2)–Cl(3)	81.7 (2)		

[a] Numbers in parentheses are estimated standard deviations in the least significant digits.

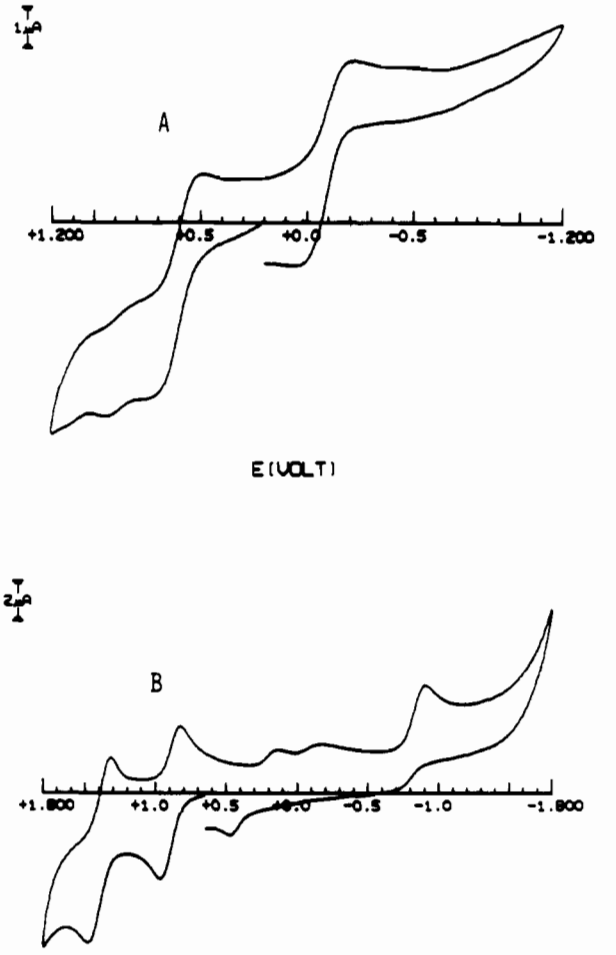

Figure 8. Cyclic voltammograms of CH_2Cl_2 solutions of (A) the C_2 isomer of compound **2** and (B) compound **1a**.

for our subsequent assessment of the other compounds. The enlarged Ru–Cl_b–Ru angles and contracted Cl_b–Ru–Cl_b angles show that there is strong repulsion between the Ru atoms, and the long Ru to Ru distances, 3.28 to 3.44 Å, can be taken as

Table XIII. Selected Bond Distances (Å) and Angles (deg) for $Ru_2Cl_5(PMe_2Ph)_4$[a]

Bond Distances			
Ru(1)-Ru(1)	2.994 (0)	Ru(1)-Cl(3)	2.359 (1)
Ru(1)-Cl(1)	2.476 (1)	Ru(1)-P(1)	2.305 (1)
Ru(1)-Cl(2)	2.391 (1)	Ru(1)-P(2)	2.305 (1)
Ru(1)-Cl(2)	2.502 (1)		

Bond Angles			
Ru(1)-Ru(1)-Cl(1)	52.80 (2)	Cl(2)-Ru(1)-Cl(3)	177.99 (4)
Ru(1)-Ru(1)-Cl(2)	53.98 (2)	Cl(2)-Ru(1)-P(1)	97.39 (4)
Ru(1)-Ru(1)-Cl(2)	50.61 (3)	Cl(2)-Ru(1)-P(2)	89.42 (4)
Ru(1)-Ru(1)-Cl(3)	124.03 (3)	Cl(2)-Ru(1)-Cl(3)	93.51 (4)
Ru(1)-Ru(1)-P(1)	127.60 (3)	Cl(2)-Ru(1)-P(1)	88.72 (4)
Ru(1)-Ru(1)-P(2)	120.20 (3)	Cl(2)-Ru(1)-P(2)	170.77 (4)
Cl(1)-Ru(1)-Cl(2)	88.92 (3)	Cl(3)-Ru(1)-P(1)	83.73 (4)
Cl(1)-Ru(1)-Cl(2)	86.44 (3)	Cl(3)-Ru(1)-P(2)	92.05 (4)
Cl(1)-Ru(1)-Cl(3)	89.81 (3)	P(1)-Ru(1)-P(2)	99.22 (4)
Cl(1)-Ru(1)-P(1)	171.68 (4)	Ru(1)-Cl(1)-Ru(1)	74.41 (4)
Cl(1)-Ru(1)-P(2)	86.21 (3)	Ru(1)-Cl(2)-Ru(1)	75.41 (3)
Cl(2)-Ru(1)-Cl(2)	84.86 (4)		

[a] Numbers in parentheses are estimated standard deviations in the least significant digits.

Table XIV. Selected Bond Distances (Å) and Angles (deg) for $Ru_2Cl_5(PMe_3)_4$[a]

Bond Distances			
Ru(1)-Ru(2)	2.992 (1)	Ru(2)-Cl(1)	2.397 (2)
Ru(1)-Cl(1)	2.385 (2)	Ru(2)-Cl(2)	2.460 (2)
Ru(1)-Cl(2)	2.455 (2)	Ru(2)-Cl(3)	2.481 (2)
Ru(1)-Cl(3)	2.473 (2)	Ru(2)-Cl(5)	2.351 (2)
Ru(1)-Cl(4)	2.348 (2)	Ru(2)-P(3)	2.290 (2)
Ru(1)-P(1)	2.309 (2)	Ru(2)-P(4)	2.273 (2)
Ru(1)-P(2)	2.290 (2)		

Bond Angles			
Ru(2)-Ru(1)-Cl(1)	51.44 (4)	Ru(1)-Ru(2)-Cl(3)	52.72 (4)
Ru(2)-Ru(1)-Cl(2)	52.58 (4)	Ru(1)-Ru(2)-Cl(5)	127.71 (5)
Ru(2)-Ru(1)-Cl(3)	52.97 (4)	Ru(1)-Ru(2)-P(3)	121.49 (5)
Ru(2)-Ru(1)-Cl(4)	128.41 (5)	Ru(1)-Ru(2)-P(4)	122.38 (5)
Ru(2)-Ru(1)-P(1)	125.01 (5)	Cl(1)-Ru(2)-Cl(2)	89.36 (6)
Ru(2)-Ru(1)-P(2)	119.51 (5)	Cl(1)-Ru(2)-Cl(3)	86.81 (6)
Cl(1)-Ru(1)-Cl(2)	89.75 (6)	Cl(1)-Ru(2)-Cl(5)	178.52 (7)
Cl(1)-Ru(1)-Cl(3)	87.25 (6)	Cl(1)-Ru(2)-P(3)	88.72 (7)
Cl(1)-Ru(1)-Cl(4)	178.34 (6)	Cl(1)-Ru(2)-P(4)	92.60 (6)
Cl(1)-Ru(1)-P(1)	92.40 (6)	Cl(2)-Ru(2)-Cl(3)	81.92 (5)
Cl(1)-Ru(1)-P(2)	88.57 (6)	Cl(2)-Ru(2)-Cl(5)	89.17 (7)
Cl(2)-Ru(1)-Cl(3)	82.19 (6)	Cl(2)-Ru(2)-P(3)	172.56 (6)
Cl(2)-Ru(1)-Cl(4)	91.20 (6)	Cl(2)-Ru(2)-P(4)	91.52 (6)
Cl(2)-Ru(1)-P(1)	173.46 (6)	Cl(3)-Ru(2)-Cl(5)	92.90 (6)
Cl(2)-Ru(1)-P(2)	91.22 (6)	Cl(3)-Ru(2)-P(3)	90.80 (6)
Cl(3)-Ru(1)-Cl(4)	91.53 (6)	Cl(3)-Ru(2)-P(4)	173.42 (7)
Cl(3)-Ru(1)-P(1)	91.74 (6)	Cl(5)-Ru(2)-P(3)	92.73 (8)
Cl(3)-Ru(1)-P(2)	172.21 (6)	Cl(5)-Ru(2)-P(4)	87.52 (7)
Cl(4)-Ru(1)-P(1)	86.52 (6)	P(3)-Ru(2)-P(4)	95.75 (7)
Cl(4)-Ru(1)-P(2)	92.77 (7)	Ru(1)-Cl(1)-Ru(2)	77.47 (5)
P(1)-Ru(1)-P(2)	95.00 (7)	Ru(1)-Cl(2)-Ru(2)	75.01 (5)
Ru(1)-Ru(2)-Cl(1)	51.09 (4)	Ru(1)-Cl(3)-Ru(2)	74.31 (5)
Ru(1)-Ru(2)-Cl(2)	52.41 (4)		

[a] Numbers in parentheses are estimated standard deviations in the least significant digits.

representative of nonbonded Ru-Ru interactions within FSBO structural context.

Turning now to the II,III compounds, we first recognize that there are three structural types. A preliminary survey of the tabulated structural data shows that those of one type, with the unsymmetrical distribution of ligands $L_3RuCl_3RuCl_2L$, differ considerably from those of the other two types where there are L_2Cl groups of ligands on both ends. The Ru to Ru distances in the two $L_3RuCl_3RuCl_2L$ molecules are long (3.28 Å), and the angles also suggest little if any attraction between the metal atoms. In fact, this Ru-Ru distance and the angles are very similar to those in the II,II complexes. On this structural basis alone, it is tempting to postulate that there is clean valence trapping in these molecules so that the one metal atom is a d^6 Ru^{II} and the other a d^5 Ru^{III}. Having said that, it is logical to go further and assign

Table XV. Selected Bond Distances (Å) and Angles (deg) for $Ru_2Cl_6(PEt_3)_3$[a]

Bond Distances			
Ru(1)-Cl(1)	2.340 (2)	Ru(2)-Cl(1)	2.588 (2)
Ru(1)-Cl(2)	2.517 (2)	Ru(2)-Cl(2)	2.406 (2)
Ru(1)-Cl(3)	2.513 (2)	Ru(2)-Cl(3)	2.406 (2)
Ru(1)-Cl(4)	2.300 (2)	Ru(2)-Cl(5)	2.313 (2)
Ru(1)-P(1)	2.335 (2)	Ru(2)-Cl(6)	2.308 (2)
Ru(1)-P(2)	2.336 (2)	Ru(2)-P(3)	2.271 (2)

Bond Angles			
Cl(1)-Ru(1)-Cl(2)	84.07 (7)	Cl(1)-Ru(2)-Cl(5)	92.06 (8)
Cl(1)-Ru(1)-Cl(3)	85.35 (7)	Cl(1)-Ru(2)-Cl(6)	91.03 (8)
Cl(1)-Ru(1)-Cl(4)	176.69 (8)	Cl(1)-Ru(2)-P(3)	175.31 (8)
Cl(1)-Ru(1)-P(1)	93.76 (7)	Cl(2)-Ru(2)-Cl(3)	82.68 (7)
Cl(1)-Ru(1)-P(2)	88.87 (8)	Cl(2)-Ru(2)-Cl(5)	172.38 (8)
Cl(2)-Ru(1)-Cl(3)	78.39 (7)	Cl(2)-Ru(2)-Cl(6)	91.86 (8)
Cl(2)-Ru(1)-Cl(4)	93.12 (8)	Cl(2)-Ru(2)-P(3)	94.92 (8)
Cl(2)-Ru(1)-P(1)	92.25 (7)	Cl(3)-Ru(2)-Cl(5)	92.90 (8)
Cl(2)-Ru(1)-P(2)	168.86 (8)	Cl(3)-Ru(2)-Cl(6)	171.99 (9)
Cl(3)-Ru(1)-Cl(4)	92.37 (8)	Cl(3)-Ru(2)-P(3)	94.51 (7)
Cl(3)-Ru(1)-P(1)	170.64 (8)	Cl(5)-Ru(2)-Cl(6)	91.87 (9)
Cl(3)-Ru(1)-P(2)	92.48 (8)	Cl(5)-Ru(2)-P(3)	91.60 (9)
Cl(4)-Ru(1)-P(1)	88.10 (8)	Cl(6)-Ru(2)-P(3)	91.78 (8)
Cl(4)-Ru(1)-P(2)	93.63 (8)	Ru(1)-Cl(1)-Ru(2)	80.85 (6)
P(1)-Ru(1)-P(2)	96.82 (8)	Ru(1)-Cl(2)-Ru(2)	81.10 (7)
Cl(1)-Ru(2)-Cl(2)	81.24 (7)	Ru(1)-Cl(3)-Ru(2)	81.17 (6)
Cl(1)-Ru(2)-Cl(3)	82.38 (7)		

[a] Numbers in parentheses are estimated standard deviations in the least significant digits.

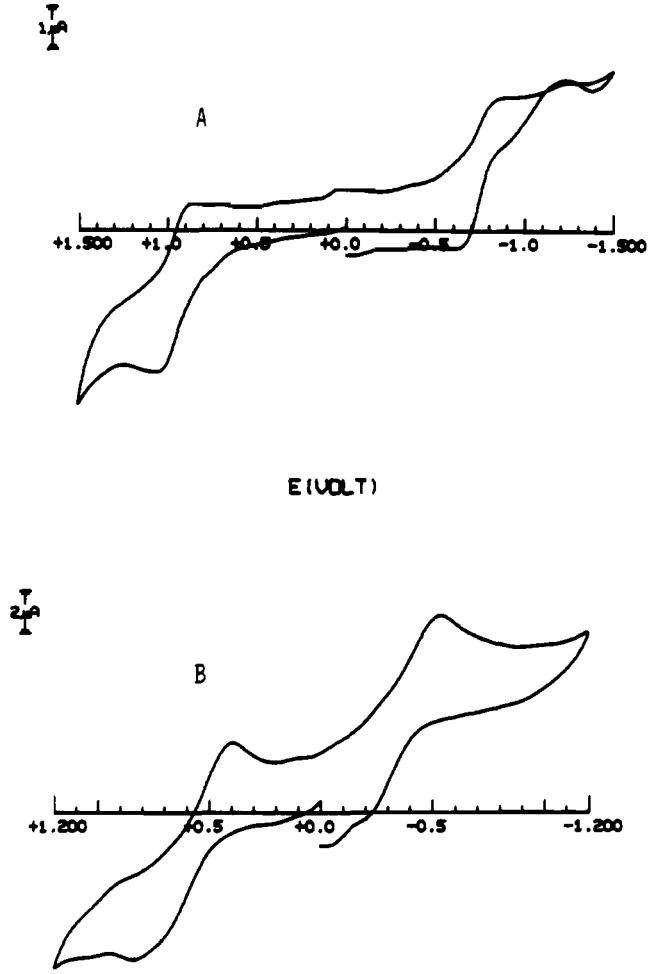

Figure 9. Cyclic voltammograms of CH_2Cl_2 solutions of (A) compound **2** and (B) compound **3**.

the Ru^{II} to the $L_3Ru(\mu\text{-}Cl)_3$ environment and the Ru^{III} to the more anionic set of ligands $(\mu\text{-}Cl)_3RuCl_2L$. This choice maximizes $d\pi$-$p\pi$ back-bonding at one end as well as favorable electrostatic interaction at the other. It will be seen later that electrochemical

Table XVI. Electrochemical and Magnetic Data for Face-Sharing Bioctahedral Ruthenium Complexes

	$E_{1/2}$,[a] V		μ_{eff},				
	[O]	[R]	μ_B/Ru_2	g_1	g_2	g_3	ref
			Ru(II), Ru(II)				
			$[L_3RuCl_3RuL_3]^+$				
L = PEt_2Ph	+1.75						8
	+1.20						
L = PBu_3	+1.39						this work
	+0.90						
			Ru(II), Ru(III)				
			$L_3RuCl_3RuCl_2L$[b]				
L = PMe_2Ph[c]	+0.81	−0.76					8
L = PEt_2Ph	+1.27	−0.28	1.83	2.46	1.63		8
L = PBu_3	+0.95	−0.73	1.95	2.44	1.59		this work
L = As(*p*-tol)$_3$[c,d]	+1.24	−0.26	2.27	2.54	1.63		8, 17
L = As(*p*-ClC_6H_4)$_3$[c]	+1.26	−0.42		2.48	1.76		8
			$L_2ClRuCl_3RuClL_2$, C_2 Symmetry				
L = PBu_3	+0.61	−0.28	1.12	2.37	2.05	1.83	9, this work
L = As(*p*-tol)$_3$[c]	+0.83	+0.10		2.41	2.11	1.87	8, 17
L = $AsPh_3$[c]	+0.90	+0.14	1.75	2.32	2.03	1.76	8
L = PMe_2Ph	+0.55	−0.09	1.94	2.33	2.06	1.87	this work
			$L_2ClRuCl_3RuClL_2$, C_{2v} Symmetry				
L = PMe_3	+0.58	−0.18		2.29	2.07	1.90	this work
			Ru(III), Ru(III)				
			$L_2ClRuCl_3RuCl_2L$				
L = PEt_3			1.91/Ru				this work
L = As(*p*-tol)$_3$[c]		+0.58	1.45/Ru				17
		−0.44					
L = $AsPh_3$[c]		+0.62					17
		−0.44					

[a] [O] = reversible one-electron oxidation occurs at this potential; [R] = reversible one-electron reduction occurs at this potential. [b] The molecule has approximate C_s point symmetry. [c] No X-ray crystal structure has been reported. [d] *p*-tol = *p*-tolyl group.

Table XVII. Selected Structural Parameters for Face-Sharing Bioctahedral Ruthenium Complexes

	Ru–Ru, Å	∠Ru–Cl_b–Ru,[a] deg	∠Cl_b–Ru–Cl_b, deg	ref
		Ru(II), Ru(II)		
		$[L_3RuCl_3RuL_3]^+$		
L = PBu_3	3.39	86.2	78.5	this work
L = PMe_3	3.28	82.9	80.9	4
L = PMe_2Ph	3.37	86.0	78.7	5
L = PEt_2Ph	3.44	87.9	77.2	6
		$L_3RuCl_3RuClL_2$		
L = PEt_2Ph	3.37	85.2	79.2	7
		Ru(II), Ru(III)		
		$L_3RuCl_3RuCl_2L$[b]		
L = PBu_3	3.28	83.6	80.4	this work
L = PEt_2Ph	3.28	82.9		8
		$L_2ClRuCl_3RuClL_2$, C_2 Symmetry		
L = PBu_3	3.12	79.4	83.5	9
L = PMe_2Ph	2.99	75.1	86.7	this work
		$L_2ClRuCl_3RuClL_2$, C_{2v} Symmetry		
L = PMe_3	2.99	75.6	86.2	this work
		Ru(III), Ru(III)		
		$L_2ClRuCl_3RuCl_2L$		
L = PBu_3	3.18	80.5	82.8	1
L = PEt_3	3.20	81.0	82.4	this work

[a] Cl_b = bridging Cl ligand. [b] The molecule has approximate C_s point symmetry.

and EPR data support the above proposal.

The other II,III complexes, which both have balanced ligand distributions and differ only in the symmetry (C_2 vs C_{2v}) have considerably shorter Ru to Ru distances (2.99, 2.99 and 3.12 Å) as well as angles indicative of less Ru–Ru repulsion. For compounds of this type, it would appear that delocalization of the unpaired electron and the existence of weak Ru–Ru bonding (formal bond order of $^1/_2$) are indicated by the structural data.

For the III,III compounds the structural data alone are inconclusive. The evidence for unmitigated Ru–Ru repulsion is not as extreme as in the II,II compounds, but the structure suggests that any Ru–Ru bonding that does exist is weak—weaker than in the symmetrical II,III compounds even though the presence of two d^5 configurations would permit the formation of a full single bond.

Electrochemical and EPR Results and Their Implications. We turn now to Table XVI with the purpose of seeing how these data may serve to support and clarify the tentative conclusions just drawn from the structural data. Once again, the II,II compounds are easily understood and provide calibration points for interpreting the results on the other classes of compounds. The pairs of oxidation potentials are related as would be expected, the second ones being considerably more positive. This may be attributed to delocalization of the charge (and the odd electron) in the symmetrical $[L_3RuCl_3RuL_3]^{2+}$ ions.

All of the II,III neutral molecules are far more easily oxidized than the $[L_3RuCl_3RuL_3]^{2+}$ dications or even the $[L_3RuCl_3RuL_3]^+$ ions, as would be expected. For the unsymmetrical $L_3RuCl_3RuCl_2L$ type compounds, there is a very large difference between the oxidation and the reduction voltages, 1.50–1.68 V. This is consistent with the trapped valence assignment based on the structural data. Oxidation takes place from a stable Ru(dπ)–P(dπ) bonding orbital on the $L_3Ru^{II}(\mu\text{-}Cl)_3$ unit, while the reduction fills a vacancy on the $(\mu\text{-}Cl)_3Ru^{III}Cl_2L$ unit, stabilized electrostatically. Hence, both oxidation and reduction are relatively difficult, and the potentials are widely separated.

For both types of $L_2ClRuCl_3RuClL_2$ molecule, the delocalization and Ru–Ru bonding result in the HOMO being a half-filled σ MO where both oxidation and reduction take place. Hence, the oxidations and reductions are closer together, viz., only 0.64–0.89 V apart.

For the III,III molecules, no oxidation wave was seen, as expected, but reduction occurs in two stages, rather well separated.

This does not give any clear indication as to how much Ru–Ru bonding may be present. However, the magnetic susceptibility data indicate that there is effectively one unpaired electron on each metal atom, although perhaps these are loosely coupled. Essentially, these III,III molecules are not metal–metal bonded.

Finally, we must comment on the remarkable and characteristic difference between the EPR spectra for the unsymmetric and symmetrical types of II,III compounds. As already noted by Stephenson and co-workers, we have here a very handy criterion for distinguishing between the two classes, although it is not possible in this way (or by CV data) to distinguish between the C_2 and C_{2v} types of $L_2ClRuCl_3RuClL_2$ compounds. The "axial" spectrum given by the $L_3RuCl_3RuCl_2L$ molecule is consistent with the proposed valence trapping since the odd electron is in an approximately axial $Ru^{III}Cl_5L$ environment. For the symmetrical molecules in which there is no symmetry axis of order > 2, the appearance of a rhombic **g** tensor is expected.

Acknowledgment. We thank the National Science Foundation for support and Dr. Larry Falvello for crystallographic assistance. We also thank Dr. George Bates for allowing R.C.T. to use the EPR spectrometer.

Supplementary Material Available: Tables of anisotropic displacement parameters and additional bond distances and angles (33 pages); listings of calculated and observed structure factors (144 pages). Ordering information is given on any current masthead page.

Contribution from the Department of Chemistry, University of the Orange Free State, Bloemfontein 9300, South Africa, and Institute for Inorganic Chemistry, University of Witten/Herdecke, 5810 Witten, FRG

Solvent, Temperature, and Pressure Dependence of the Oxidative Addition of Iodomethane to Complexes of the Type $Rh^I(\beta\text{-diketonate})(CO)(PPh_3)$

J. A. Venter,[1a] J. G. Leipoldt,*[,1a] and R. van Eldik*[,1b]

Received October 4, 1990

A combined solvent-, temperature-, and pressure-dependence study of the oxidative addition of iodomethane to Rh(Sacac)-(CO)(PPh_3) and Rh(cupf)(CO)(PPh_3) was undertaken for a range of solvents covering a large range of ϵ_0 and q_p values. The kinetic data for the thioacetylacetone (Sacac) complex exhibit no significant dependence on the solvent and are interpreted in terms of a concerted three-center transition state. In the case of the cupferron (cupf) complex, a significant solvent effect was observed for the most polar solvents. This observation is interpreted in terms of a linear transition state and the participation of an ion-pair intermediate at least in the case of the polar solvents. The results are discussed in reference to all the data available in the literature for such reactions.

Introduction

Oxidative-addition reactions of alkyl halides to transition-metal complexes are of general importance in terms of the formation of metal alkyl and metal acyl species and their role in catalytic processes.[2-4] We are especially interested in the mechanistic behavior of β-diketone and related complexes of Rh(I) and Ir(I) because of the possibility to support these complexes on a polymer like polystyrene and so heterogenize the potentially homogeneous catalysts.

We have in recent years investigated the kinetics of the oxidative addition of iodomethane to complexes of the type Rh(LL)-(CO)(PX_3) and Rh(LL)(PX_3)$_2$, where LL = β-diketones and cupferron and X = phenyl, *p*-chlorophenyl and *p*-methoxyphenyl.[5-10] Solvent and pressure effects[9-11] were studied in order to obtain more information on the nature of the transition state in terms of I (for a concerted three-centered mechanism) or II (for a S_N2 mechanism). For the oxidative addition of CH_3I to

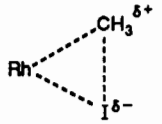

I

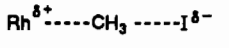

II

$Ir(Cl)(CO)(PPh_3)_2$,[11] the volume of activation exhibited a good correlation with the solvent parameter q_p,[12] from which it was concluded that a linear transition state (II) is more in accordance with the measured $\Delta V^{\ddagger}$ data than the concerted three-center state (I).[11] In our earlier studies, some solvent effects were observed,[8-10] but data for a wide range of solvents in terms of ϵ and q_p values were lacking and prevented a detailed interpretation.

In this study, we have now investigated the solvent, temperature, and pressure dependence of reactions 1 and 2 for a series of

$$Rh(Sacac)(CO)(PPh_3) + CH_3I \rightarrow Rh(Sacac)(COCH_3)(I)(PPh_3) \quad (1)$$

$$Rh(cupf)(CO)(PPh_3) + CH_3I \rightarrow Rh(cupf)(CO)(CH_3)(I)(PPh_3) \quad (2)$$

solvents, where HSacac = thioacetylacetone, $CH_3C(S)CH_2C(O)CH_3$, and cupf = cupferron, $C_6H_5N(OH)NO$. The product in the case of reaction 1 is the acyl complex, whereas the alkyl

(1) (a) University of the Orange Free State. (b) University of Witten/Herdecke.
(2) Parshall, G. W.; Mrowca, J. J. *Adv. Organomet. Chem.* **1968**, *7*, 157.
(3) Roth, J. F.; Craddock, J. H.; Hershman, A.; Paulik, F. E. *Chem. Technol.* **1971**, 600.
(4) van Koten, G.; Terheijden, J.; van Beek, J. A. M.; Wehman-Ooyevaar, I. C. M.; Muller, F.; Stam, C. H. *Organometallics* **1990**, *9*, 903.
(5) Basson, S. S.; Leipoldt, J. G.; Nel, J. T. *Inorg. Chim. Acta* **1984**, *86*, 167.
(6) Basson, S. S.; Leipoldt, J. G.; Roodt, A.; Venter, J. A.; van der Walt, T. J. *Inorg. Chim. Acta* **1986**, *119*, 35.
(7) Basson, S. S.; Leipoldt, J. G.; Roodt, A.; Venter, J. A. *Inorg. Chim. Acta* **1987**, *128*, 31.
(8) Leipoldt, J. G.; Basson, S. S.; Botha, L. J. *Inorg. Chim. Acta*, in press.
(9) Leipoldt, J. G.; Steynberg, E. C.; van Eldik, R. *Inorg. Chem.* **1987**, *26*, 3068.
(10) van Zyl, G. J.; Lamprecht, G. J.; Leipoldt, J. G.; Swaddle, T. W. *Inorg. Chim. Acta* **1988**, *143*, 223.
(11) Stieger, H.; Kelm, H. *J. Phys. Chem.* **1973**, *77*, 290.

(12) q_p is the pressure derivative of the solvent parameter $q = (\epsilon - 1)/(2\epsilon + 1)$, i.e. $q_p = [3/(2\epsilon + 1)^2](\partial\epsilon/\partial p)$, where ϵ is the dielectric constant of the solvent.

0020-1669/91/1330-2207$02.50/0